2009-01-01

Fabrication And Characterization Of Zirconium Oxide Thin Films

Vemnkata Rama Sesha Ravi Kumar Vemuri
University of Texas at El Paso, vrvemuri@miners.utep.edu

FABRICATION AND CHARACTERIZATION OF ZIRCONIUM OXIDE THIN FILMS

VENKATA RAMA SESHA RAVI KUMAR VEMURI

Department of Electrical and Computer Engineering

APPROVED:

Ramana. V. Chintalapalle, Ph.D., Co-Chair

David Zubia, Ph.D., Co-Chair

Eric MacDonald, Ph.D.

Miguel Castro-Colin, Ph.D.

Patricia D. Witherspoon, Ph.D.
Dean of the Graduate School

Dedicated

In fond memory of my beloved father

Sri Rama Murthy Vemuri

FABRICATION AND CHARACTERIZATION OF ZIRCONIUM OXIDE THIN FILMS

by

VENKATA RAMA SESHA RAVI KUMAR VEMURI, B.TECH

THESIS

Presented to the Faculty of the Graduate School of

The University of Texas at El Paso

in Partial Fulfillment

of the Requirements

for the Degree of

MASTER OF SCIENCE

Department of Electrical and Computer Engineering

THE UNIVERSITY OF TEXAS AT EL PASO

December 2009

Acknowledgements

I would like to thank my advisor Dr. Chintalapalle V. Ramana for his guidance, encouragement, support without which this thesis is not possible. I feel that he exposed me to frontier research areas and was keen through this research and was very helpful in solving research problems. I was very thankful to him.

I was also thankful to Dr. David Zubia for giving me opportunity join Nano Materials Integration Laboratory (NanoMIL) research group. The courses taught by him are very helpful in grasping the fundamentals of semiconductor technology and pursue this research all along.

I would also extend my thanks to Dr. John McClure for all his encouragement and helpful discussions during this thesis work.

I am very thankful to all my NanoMIL research members Rafa, Brandon, Ivan, Arev, Oscar, Jose and all other members for all their support, research and laboratory knowledge I gained from these while performing this work.

I would be grateful for Dr. MacDonald and Dr. Castro colins for being on my committee and reviewing my thesis work. I would also like to thank my research team members Satya, Narasimaha Raju, Franscisco, Nydia and Victoria for the help in this research project.

I take this opportunity to acknowledge and thank the Air Force Research Laboratory for the partial financial support to perform some portions of this work for a research grant that Dr. Ramana, my thesis advisor, has been directing here at the University of Texas at El Paso (UTEP). I am sure that I would not have been able to finish my M.S. degree without that financial support. Partial financial support from the University Research Initiate (URI) minor grant for Dr. Ramana to purchase some materials and initiate research programs in the topical area of Zr and Hf based advanced electronic and optical materials at UTEP is also acknowledged with appreciations. I would also extend my sincere thanks to the Department of Electrical and Computer Engineering for providing early financial assistance in the form of Teaching Assistantship.

Finally I would like to thank all my family, friends and staff of college of engineering who directly or indirectly helped me to complete this research work. I am proud to mention that I am the very

first M.S. graduate in my family and I look forward to my exciting career. I would not have had this opportunity to pursue M.S. without a constant support from my family.

Abstract

Zirconium oxide (ZrO_2) is an important material with a potential for a wide range of technological applications. The outstanding chemical stability, electrical and mechanical properties, high dielectric constant, and wide band gap of ZrO_2 make it suitable for several industrial applications in the field of optics, electronics, magneto-electronics, and optoelectronics. ZrO_2 is frequently used as a high refractive index material in multilayer optical coatings in high power laser systems. ZrO_2 is employed in super plastic structural ceramics that demonstrate excellent strength and fracture toughness. ZrO_2 has been considered as a promising dielectric to replace SiO_2 in advanced metal oxide semiconductor (MOS) devices in gate stack. In addition, ZrO_2 exhibits functionality in the ultraviolet regions of the electromagnetic spectrum. If the properties can be tuned, it can become a useful candidate for all applications in the desired regions of the electromagnetic spectrum. However, it is well known that the electrical and optical properties of ZrO_2 thin films are highly dependent on the film-substrate interface structure, morphology, and chemistry, which are in turn controlled by the film-fabrication technique, growth conditions, and post-deposition processes.

The goal of present work is to grow and demonstrate the high quality of ZrO_2 thin films for application in electronic and optoelectronic devices. The specific objectives of the work are: (1) grow ZrO_2 films under varying growth conditions using radio frequency (RF) magnetron sputtering, (2) gain a better understanding of the growth and local structure, interface structure and chemical reactions at the ZrO_2-Si interface for ZrO_2 films grown on Si (100) substrates, (3) study the material properties and (4) optimize the conditions to produce high quality ZrO_2. In the present work, ZrO_2 thin films have been prepared by the radio-frequency magnetron sputter-deposition onto Si (100) substrates as a function of growth temperature (T_s) varied in a wide range of 30-400 ^oC.

The growth behavior, surface structure, morphological features, interface structure, and chemical analysis of surfaces and interfaces have been examined by the high-resolution transmission electron

microscopy (HRTEM) and high-resolution scanning electron microscopy (HR-SEM). The crystal structure and interface analysis have been performed using x-ray diffraction (XRD) and x-ray reflectivity (XRR). The optical and electrical properties were evaluated by studying the optical absorption and capacitance-voltage measurements, respectively. The results indicate that the effect of T_s on the surface structure, interface layers and morphology of ZrO_2 films is significant. ZrO_2 films grown at 30 ^oC are nanocrystalline without an interface layer (IL) formation. An increase in T_s results in the improvement in the crystallinity of ZrO_2 films. The grain sizes determined were in the range 5-40 nm, where the temperature-dependence is clear. Similarly, it was found that the effect of T_s is significant on the optical band gap and dielectric constant of ZrO_2 films. Efforts are made to explain the quantitative information, obtained based on the electron microscopy results, making use of the existing models to account for growth behavior and interface structure.

Table of Contents

List of Tables

List of Figures

Chapter 1: Introduction

1.1 Scaling and Current CMOS technology

For four decades, complementary metal oxide semiconductor technology (CMOS) has been the driving force behind continued development of information technology, telecommunications and supercomputing. All improvements pertaining to current computing infrastructure are achieved through continuously improving performance of the Integrated Circuit (IC) chips. This improved performance of IC's can be attributed to scaling of its fundamental building block, the MOSFET (Metal Oxide Semiconductor Field Effect Transistor). Scaling is the reduction in device (MOSFET) dimensions, so as to increase the integration density and reduce the power consumption. With scaling more devices can be packed into the same die size. In the 1960's Gordon Moore, the founding chairman of Intel corp., predicted that the number of devices on an integrated circuit increases exponentially for every 2-3 years [1]. This became known as Moore's law. Scaling, since then, has reduced the device dimensions feature size [2]. The current channel length of a MOSFET is 45nm. The current gate oxide thickness is 1.6 nm.

Scaling involves systematic reduction of MOS device dimensions so that the reduction in the MOSFET dimensions will affect the operating characteristics of the MOSFET. In simple, the scaling phenomenon can be explained in terms of mathematical relations.

Scaling, in which electric fields inside MOSFET were kept constant, is called constant field scaling. In order to keep the electric field constant, the gate oxide thickness (t_{ox}) is scaled down by a factor of S and oxide capacitance was changed as follows,

$$C'_{ox} = \frac{\varepsilon_{ox}}{t'_{ox}} = S\frac{\varepsilon_{ox}}{t_{ox}} = SC_{ox} \quad (1.1)$$

The drain current (I_D) and drain to source voltage (V_{DS}) are also scaled down accordingly as follows,

$$I'_D = \frac{I_D}{S} \text{ and } V'_{DS} = \frac{V_D}{S} \quad (1.2)$$

Then the power dissipation (P) is scaled down by a factor of S^2,

$$P' = V'_{DS} I'_D = \frac{1}{S^2} I_D V_{DS} = \frac{P}{S^2} \quad ---------- (1.3)$$

All the primed quantities are tkhe scaled down quantities of the MOSFET parameters.

As indicated by Eq 1.3, constant electric field scaling reduces power dissipation by a factor of S^2. Interestingly, scaling successfully continued for four decades and MOSFET technology evolved continuously. It is to be noted that, with scaling, the gate oxide thickness also scaled down accordingly. However, the continued scaling imposed physical limitations on the gate oxide thickness. A detailed discussion will be made in section 1.2 about the complications of ultra thin gate oxide.

1.2 SiO_2 as traditional gate dielectric and future challenges

For the past four decades, SiO_2 served as excellent gate dielectric. The characteristics that made SiO_2 an excellent gate dielectric are high band gap (of 9 eV)**,** a large conduction band offset with poly-Si and the silicon**,** its amorphous nature**,** its high thermal stability with substrate Si and its ease of processing and integration. SiO_2 can be grown by thermal oxidation.

Continued CMOS eventually required an ultrathin gate oxide i.e., SiO_2. Current CMOS fabrication technology requires a gate oxide thickness is of 1.5-2nm. However, ultrathin SiO_2 dielectrics pose several challenges for semiconductor industry in the near future. The very important consideration for the ultrathin SiO_2 was the leakage current (Figure 1.1). As the thickness of SiO_2 reduces the tunneling probability of electron across oxide–Si boundary increases. As per quantum mechanics, considering the tunneling probability through a potential barrier is given by [4]

$$T = \frac{4E(E - V_0)}{V_0^2 \sin^2(k_2 a) + 4E(E - V_0)} \quad ---------- (1.4)$$

where, E is the energy of the electron in eV, V_0 is the potential barrier in eV, and k_2 is the wave number. The tunneling probability of electron increases static leakage current which increases standby power consumption.

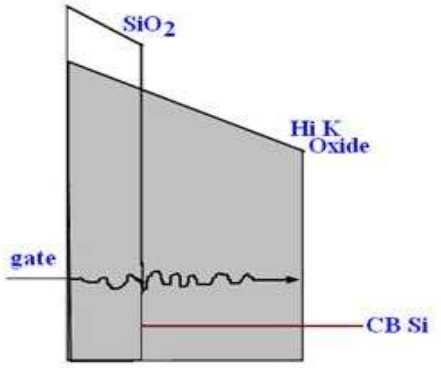

Figure 1.1: Tunneling through the gate oxide

The ultrathin SiO_2 is prone to breakdown due to hot carrier injection. In present MOSFET technology of constant voltage scaling, very high accelerating voltages exists across the ultrathin SiO_2 in the channel region. The electrons and holes in the channel region of MOSFET (called hot carriers) can gain very high kinetic energies under the influence of these fields and will be injected into the gate oxide. The injected carriers form traps in SiO_2 (Figure 1.2 [5]) and over time could create a complete conduction path across and gate and channel. This gate oxide breakdown phenomenon poses a threat to the suggested 10 year reliability of MOS devices.

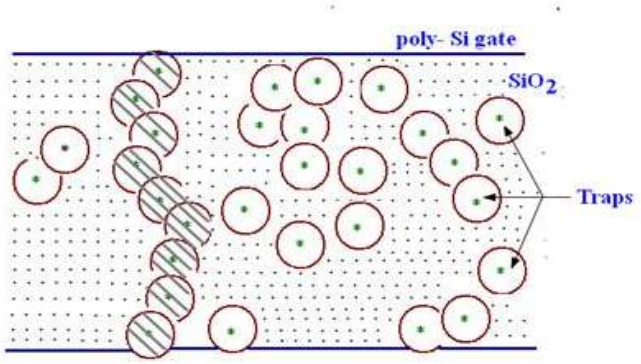

Figure 1.2: Oxide breakdown mechanisms

1.3 High-κ dielectrics

The possible solution for issues caused by scaling to ultrathin gate oxide could be replacing the SiO_2 with thicker high-κ dielectric oxide. The concept of thicker high–κ dielectric can be understood using Effective Oxide Thickness (EOT).

In simple terms, the gate oxide capacitance can be expressed as

$$C = \frac{\varepsilon_o \kappa A}{t} \quad ------- (1.5)$$

where, κ is the dielectric constant of gate oxide, *t* is the thickness and *A* is the area of MOS gate stack. For SiO_2, κ =3.9, gate oxide t_{ox} can be expressed as eq (1.6)

$$t_{ox} = 3.9\varepsilon_o \frac{A}{C} \quad ----- (1.6)$$

For high – κ material

$$t_{high-\kappa} = \kappa_{high-\kappa}\varepsilon_o \frac{A}{C} ---------- (1.7)$$

In equations (1.7) and (1.8) high κ gate oxide thickness can be expressed in terms of equivalent oxide thickness

$$t_{ox} = EOT = \frac{3.9}{\kappa_{high-\kappa}} t_{high-\kappa} \quad ---------(1.8)$$

For example, 10 nm of ZrO_2 with k=25 can have EOT=1.56 nm, which means an ultrathin SiO_2 (t_{ox}= 1.56 nm) can be replaced by a 10 nm thick high–κ oxide.

The concept of replacing SiO_2 with a high–κ oxide looks pretty simple but in reality it is extremely challenging. It was confirmed that, SiO_2 is still an excellent dielectric, with the exception of its thickness related problems. The new gate oxide candidate should mimic all of the silicon dioxide's advantages with none of its disadvantages (particularly, thickness related problems). There are issues that need to be addressed before introducing a prospective gate oxide candidate in CMOS process technology. The key issues identified are:

1) The ability to continue scaling to lower EOTs
2) The instabilities caused by the high defect densities and traps
3) Loss of carrier mobility in Si channel due to interfacial layer formation
4) Integration of gate oxide fabrication in MOS process technology

1.4 Choice of high–κ oxide

SiO_2 is the best gate oxide so far. The key advantage is fabrication of SiO_2 by thermal oxidation. SiO_2 is amorphous, has very low defect density, and forms an excellent interface with Si. In section 1.3, the characteristics of silicon dioxide, which made it the best gate oxide candidate, were discussed. The gate oxide that can replace SiO_2, therefore, must satisfy the following requirements.

1. Its dielectric constant should be high and should have a large band gap
2. The oxide should be thermodynamically stable with respect to Si channel
3. It must be kinetically stable under very high processing temperatures
4. Must be a good insulator and has high band offsets with respect to Si
5. Must form good electrical quality interface

6. Must have low defect densities

Each of these desired characteristic will be discussed in detail in the following sub sections.

1.4.1 The dielectric constant and band gap

For the successful scaling of gate oxides in foreseeable future, the κ value should be 20-30. Several lanthanide and transition metal oxides, silicates, and oxynitrides satisfy this condition. However, for many of those candidates, there exists a tradeoff between band gap and κ value. This was illustrated in Table 1.1. For example, strontium titanate, a pervoskite oxide, has a very large dielectric constant but its band gap was 3.2 eV only. Similarly, alumina has the band gap of 8.8 eV (nearly equals SiO_2) but has a fairly low dielectric constant. Out of all these oxides HfO2, ZrO_2, La_2O_3, and TiO_2 won the band gap - κ tradeoff.

Table 1.1: Comparison of several proposed gate oxide candidates

Material	κ	Band gap in eV	CB offset in eV	VB offset in eV
SiO_2	3.9	9	3.5	4.4
Al_2O_3	9	8.8	2.8	4.9
Ta_2O_5	22	4.4	0.35	3.0
ZrO_2	25	5.8	1.5	3.3
HfO_2	25	5.8	1.4	3.4
La_2O_3	30	6	2.3	3.6
TiO_2	80	6	0	5
$SrTiO_3$	3000	3.2	0	2.2

1.4.2 Thermodynamic stability

The high-κ gate oxide should not react with Si to form either SiO_2 or metal silicide. However, a chemical equilibrium exists between metal oxide and substrate silicon resulting in interfacial layer formation. The resulting SiO_2 layer would increase EOT and negate the effect of using high–κ oxide. In addition, any metallic silicide formed would be metallic and will create an electrical short through the channel.

$$MO_2 + Si \quad == \quad M + SiO_2$$

$$MO_2 + 2Si \quad == \quad MSi + SiO_2$$

where M is metal atom in proposed alternative gate oxide

This condition requires the oxide have a heat of formation higher than SiO_2 [6]. From the thermodynamic data of Al_2O_3, ZrO_2, HfO_2, Y_2O_3, and La_2O_3, it is found that these oxides are favorable candidates for SiO_2 replacement as high-κ dielectric.

1.4.3 Crystalline or amorphous nature

SiO_2 is a very good glass former and completely amorphous insulator. The same behavior was expected from the alternative gate dielectrics. It was proposed that all alternative gate electric candidates are polycrystalline and an argument existed that, grain boundaries in crystalline oxides offer leakage paths across gate oxides. It is later proved that leakage currents of amorphous and nano-crystalline oxides are the same [7].

1.4.4 Interface quality

The oxide is in direct contact with the Si channel. The channel carriers flow within the few angstroms vicinity of oxide/Si. The interface boundary between oxide and Si should be abrupt and as thin as possible. The primary advantage of SiO_2 lies in here. In case of any proposed alternative gate dielectrics, all those oxides are nano-crystalline and grain boundaries along the oxide/ Si could introduce defects and dangling bonds. For this reason it is imperative to control the interfacial layer thickness.

For many binary oxides, oxygen rapidly diffuses through silicon during RTA (rapid thermal anneal) reacting with Si, leaving interstitial defects [8] across Si. Oxygen diffusion can be controlled using surface nitridation of Si. Nitrogen acts as a barrier for oxide diffusion and reduces concentration of reactive sites for chemically active species such as O_2, O, and Si.

1.4.5 Band offset

The dielectric high-κ oxide must act as insulator. This requires that the potential barrier at each band must be over 1 eV in order to inhibit Schottky emission of carriers (Figure. 1.3) from the silicon. Table 1.1 illustrates what made the SiO_2 as a best gate dielectric for four decades. It has the highest band gap and has CB and VB offsets which are high and balanced to each other. For instance, TiO_2 has high κ value but poor CB offset, even though it is quite stable with Si and has a very high dielectric constant of 80 [7]. Referring to the Table 1.1, HfO_2 and ZrO_2 are suitable oxides as high-κ dielectric candidates.

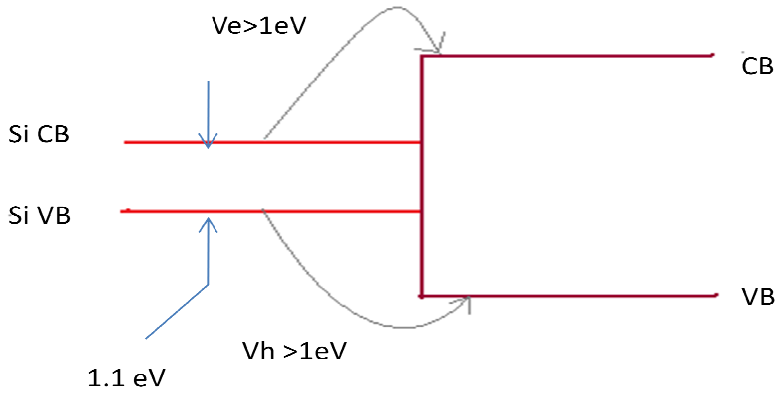

Figure 1.3: Schematic of band offsets determining carrier injection in oxide band states

By examining all the required conditions of dielectrics, it is concluded that ZrO_2 and HfO_2 are the most viable candidates for alternative high–κ dielectrics and in this thesis work research done to validate ZrO_2 as high-κ dielectric.

Chapter 2: Zirconium Oxide as a high-κ Dielectric and Previous Work

Zirconium oxide, which is the only stable oxide in the Zr-O system, is a versatile oxide material with excellent mechanical, optical, and electronic properties. These properties make zirconium oxide an important oxide material which has potential applications in domestic, industrial and military environment. There is a tremendous interest in understanding the materials and electronic properties of ZrO_2 and other Zr-based compounds. A brief discussion of ZrO_2 characteristics and materials properties will be presented in following sections.

2.1 Materials properties of ZrO_2 and application as high-κ dielectric

The key material properties of ZrO_2 includes high melting point of 2400 ^oC, high density of 5.83 g/cm^3, chemical inertness, a high fracture toughness of 17.2 $MPa.m^{0.5}$ [9], and a micro hardness of 700 (Vickers scale) [10]. ZrO_2 is an optically transparent and has a moderately low refractive index of 2-2.5 over a visible spectrum of electromagnetic radiation. This property makes it a special contender for optical applications. The three structural phases in which ZrO_2 can exist are: monoclinic (low temperature < 1000 ^oC), tetragonal (intermediate range 1000 ^oC – 2200 ^oC) and cubic phase (high temperatures > 2200 ^oC). The crystal phase will affect the materials properties of ZrO_2. This property was exploited in temperature specific applications. For example, only cubic zirconia will be used as high temperature ceramic coating.

2.2 Zirconium oxide as high–k dielectric

For several decades, ZrO_2 was found in applications such as ceramics, refractory materials, hard coatings etc. Recently, ZrO_2 was scrutinized for application in the electronic industry as promising candidate for replacing SiO_2 as gate oxide, because of its electronic properties. In addition, it has the

excellent ability to respond or filter some specific portions of the electromagnetic spectrum, a desired characteristic for use in next-generation optoelectronic devices.

ZrO_2 meets all the stringent requirements as high–κ dielectric such as:

- High dielectric constant of 25.
- Band gap of 5.8 eV and Conduction band offset of 1.3 eV [13] [14].
- Thermodynamic stability [7] [15].

2.2 Previous work

Many researchers in the industry and academia have performed research in establishing ZrO_2 as a high–κ gate dielectric. It was reported that the ZrO_2 thin films can be deposited using several techniques, such as, atomic layer deposition (ALD), chemical vapor deposition (CVD), pulsed laser deposition (PLD) and physical vapor deposition (including sputtering and e-beam deposition) [11-13]. A brief account of previous research work is as follows.

Kulki et al. [14] deposited ZrO_2 films by exploiting several organo-metallic precursors in metal oraganic chemical vapor deposition (MOCVD) method, at substrate temperatures ranging from 180 to 600 ^oC. From XRD studies, it was found that the growth at lower temperatures results in amorphous films. For intermediate temperatures, tetragonal ZrO_2 films were formed. At higher temperatures, the films were a mix of tetragonal and monoclinic phases. The calculated dielectric constant (from C-V curves) was 13-15 at lower temperatures and reached up to 19 at higher growth temperatures. This study concludes growth temperature affects crystal structure of thin films. Similar work was also reported by Cassir and his co-researchers [15]. In their work it is revealed that the deposition temperature affects growth kinetics (i.e., film thickness), crystal structure and surface morphology.

Chatterji et al. [16] demonstrated plasma enhanced CVD deposition of ultra thin ZrO_2 films with effective oxide thickness 28 Å and electrically characterized the films. High frequency C-V measurements revealed a hysteresis behavior. Flipescu [17] and Sahiner [18] separately investigated

deposition and materials properties of HfO_2 and ZrO_2 thin films fabricated by pulsed laser deposition (PLD). Sahiner investigated the effect of substrate temperature on crystalline nature of HfO_2 thin films using x-ray absorption fine structure spectroscopy (XAFS). Flipescu et al. were able to deposit smooth amorphous films. Sawa et al. [19] deposited ZrO_2 thin films using radio frequency reactive sputter deposition with varying Ar/O_2 partial pressure ratio. XRD spectra of the films deposited revealed that the films were amorphous.

Zhao et al. [20] deposited ZrO_2 films on Si (100) using reactive RF sputtering with Ar : O_2 flow ratio of 20 sccm : 8.6 sccm. The films were deposited at room temperature. XRD spectra showed monoclinic zirconia phase for thin films, and tetragonal phase was observed with the increase in thickness. The XPS spectra revealed that the films were oxygen deficient.

Chio et al. [21] studied the effect of post deposition annealing on interfacial composition and surface morphology of zirconia films. ZrO_2 films were deposited using reactive sputter deposition in $Ar+O_2$ reactive gas ambient and were annealed after deposition at temperature range of 450-750 ^{0}C. The interface layer thickness was increased with an increase in annealing temperature. X-ray photo emission spectroscopy (XPS) data showed $ZrSiO_4$ is formed at the interface with $ZrSi_x$ layer between ZrO_2 and $ZrSiO_4$.

2.3 Scope of the present work and objectives

From the above discussion, it is clear that the substrate temperature during deposition can affect the material and electronic properties of the ZrO_2 films. However, a complete and detailed analysis of the effect of the temperature on the structure and associated nano-scale phenomena have not been explored much. Furthermore, examining the structure and properties of zirconia films at the reduced dimensions is very important and can provide additional opportunities to use these materials in various emerging technological applications.

ZrO_2 has been considered as a promising dielectric to replace SiO_2 in advanced MOS devices gate stack. In addition, ZrO_2 exhibits functionality in the ultraviolet regions of the electromagnetic spectrum. If the properties can be tuned, then it can become a useful candidate for optical applications in the desired regions of the electromagnetic radiation. However, it is well known that the electrical and optical properties of ZrO_2 thin films are highly dependent on the film-substrate interface structure, morphology, and chemistry, which are in turn controlled by the film-fabrication technique, growth conditions, and post-deposition processes. Therefore, an attempt has been made in this work to study the effect of substrate temperature on the growth, microstructure, and materials properties such as ZrO_2-Si interface structure and composition, surface morphology, crystal structure, optical band gap using advanced analytical instruments.

The goal of present work is to grow and demonstrate the high quality of ZrO_2 thin films for application in electronic and optoelectronic devices. The specific objectives of the work are: (1) grow ZrO_2 films under varying growth conditions using radio frequency (RF) magnetron sputtering, (2) gain a better understanding of the growth and local structure, interface structure and chemical reactions at the ZrO_2-Si interface for ZrO_2 films grown on Si (100) substrates, (3) study the material properties and (4) optimize the conditions to produce high quality ZrO_2. In the present work, ZrO_2 thin films have been prepared by the radio-frequency magnetron sputter-deposition onto Si (100) substrates as a function of growth temperature (T_s) varied in a wide range of 30-400 ^{0}C.

The growth behavior, surface structure and morphological features, interface structure, and chemical analysis of surfaces and interfaces have been examined by the high-resolution transmission electron microscopy (HRTEM) and high-resolution scanning electron microscopy (HR-SEM). The crystal structure and interface analysis have been performed using x-ray diffraction (XRD) and x-ray reflectivity (XRR). The optical and electrical properties were evaluated by studying the optical absorption and capacitance-voltage measurements, respectively. The results indicate that the effect of T_s

on the surface structure, interface layers and morphology of ZrO_2 films is significant. ZrO_2 films grown at 30 ^oC are nanocrystalline without an interface layer (IL) formation. An increase in T_s increases grain size (up to 30 nm), where the temperature-dependence is clear. Similarly, it was found that the effect of T_s is significant on the optical band gap and dielectric constant of ZrO_2 films. The details are discussed in Chapter 4.

Chapter 3: Experiments

The zirconium oxide thin films and Metal Oxide Semiconductor (MOS) structures were fabricated in this research using carefully crafted experimental procedures. First, the substrates on which these films and devices were fabricated were cleaned thoroughly using standard laboratory cleaning procedures. The substrates used in this research were silicon (Si) and quartz. ZrO_2 films were deposited onto Si and quartz substrates using Radio Frequency (RF) magnetron sputtering. The films were characterized with advanced analytical techniques and instruments to get an insight into materials and optical properties. MOS device structures were fabricated, first depositing ZrO_2 on Si substrates and then depositing Aluminum (Al) as a top metal contact on to the ZrO_2 films. The MOS structures were further characterized performing C-V electrical measurements. All these experimental procedures and techniques are detailed in following sections.

3.1 Substrate preparation

The substrates used for all the experiments were p-type Si (100) wafers with the measured sheet resistance of 1.3 – 10 Ω-cm (measured by four point probe technique). Quartz and glass substrates were used in some of experiments. In order to avoid contamination during deposition and to achieve high performance of devices fabricated, the silicon wafers are cleaned with RCA cleaning procedure to remove organic, inorganic and metal particulate contaminants. The procedure has three major steps:

- SC1- Removal of insoluble organic contaminants using 5:1:1 $H_2O/H_2O_2/NH_4OH$ solution
- SC2- Removal of ionic and heavy metal atomic components using a solution of 5:1:1 $H_2O/H_2O_2/HCl$ solution
- Removal of native oxide by buffered oxide etches solution.

The SC1 solution was prepared by heating 50 ml of Deionized water (DI) water to a temperature of 100 ^oC and then adding each 10 ml of NH_4OH and H_2O_2 to the DI water. SC2 solution was prepared

by 10ml each of H_2O_2 and HCl to 50ml of water. The silicon substrates were soaked for 10 min in each solution and followed by 5 min of DI water rinse after each soak. Finally the silicon substrates were treated with BOE to remove any native oxide on it.

The Glass and quartz substrates were used in some experiments, especially optical characterization, along with silicon substrates. These substrates were cleaned in an ultrasonic bath of methanol (semiconductor grade), acetone (semiconductor grade), and DI water. The ultrasonic cleaning was carried out for 10min in each step followed by a DI water rinse and then dried with nitrogen.

3.2 Thin film deposition

ZrO_2 thin films were deposited using a radio frequency magnetron sputtering, which is a method of physical vapor deposition.

The sputter process involves bombardment of target material by ionized atoms, usually Ar+ ions. The target material (called sputter target) material is placed on a cathode and a negative voltage is applied to the cathode. The chamber is evacuated to high vacuum, usually; 10^{-6}Ttorr and Ar gas will be injected into chamber at low pressures. The Ar gas will be ionized to create Ar^+ plasma. Ar+ ions accelerate towards cathode, under the influence of cathode voltage, and bombard the target ejecting a target atom. The target atom will be deposited on to the substrate placed above the target. In this research RF magnetron sputtering was employed. In this type of sputtering a radio frequency voltage of 13.56 MHz was applied to the target and the sputter cathode was equipped with a magnet.

Nano Materials Integration Laboratory at The University of Texas at El Paso was equipped with Kurt J Lesker Company made sputtering chamber. A brief discussion of its characteristics and capabilities will be discussed in section 3.2.1.

3.2.1 Description of KJLC sputtering deposition system

The magnetron sputtering system (Kurt.J.Lesker company) is a high vacuum system equipped with two 2" and one 3" magnetron sputtering sources. A 3 KW e-beam deposition capability was also integrated into the same system. The substrate holder can accommodate 5 substrates at a time for batch processing.

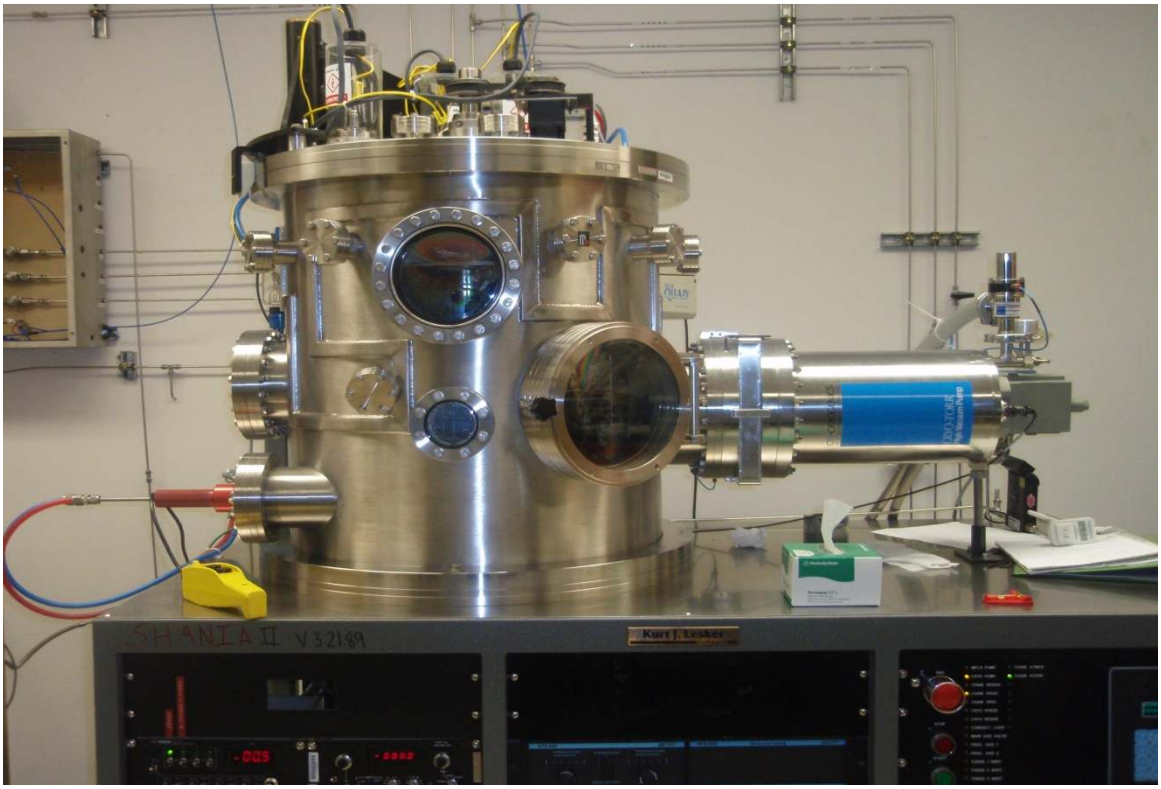

Figure 3.1: Kurt J Lesker high vacuum thin film deposition systems

KJLC system has a multiple gas injection system which can accommodate a precise injection and control of 4 different gases. Accurate reactive gas flow can be achieved and monitored by four channel configuration of MKS 247D four channel readout, MKS 250E pressure controller, MKS Baratron pressure transducer and MKS 1100 mass flow controllers. The chamber was fitted with a 500W

tungsten – halogen heater lamp assembly which can heat the substrate to 600 ^{o}C. The chamber is fitted with Edwards E2M28 rotatory vane oil pump (rough vacuum pump) and Helix- technology CRYO TORR 8 cryo pump for vacuum creation inside the chamber. The rough vacuum pump can create a vacuum of 200 mTorr of vacuum which is the crossover point of CT-8 cryo pump. The combination of rough and cryo pumps could achieve up to $3x10^{-7}$ Torr of ultimate vacuum. The chamber is water cooled and is equipped with advanced energy RFX-600 Radio Frequency (RF) power supply and ATX – 600 reactive power control tuner circuits. The RF power supply is capable of supplying 600 W of RF power at 13.56 MHz. The RF power supply is connected to TORUS 2C sputter cathode. TORUS 2C is 2" circular sputter cathode which is capable of RF, DC, Pulsed DC power operations.

3.2.2 Deposition of ZrO_2 films

ZrO_2 films were deposited at various substrate temperatures to study effect of substrate temperature on the growth behavior, surface morphology, crystal structure and ZrO_2/Si interface structure. The chamber is evacuated for a base pressure of $5x10^{-7}$ Torr. Ar gas was injected into the chamber at a flow rate of 50sccm and at 2.8 mTorr of pressure. Throughout all the experiments the pressure was kept constant. 2" diameter zirconium oxide sputtering target (99.99% pure) was used. The sputtering conditions are summarized in Table 3.1.

For optical characterization, especially optical transmission measurements, it was later found that quartz as the substrate material will be good. So the depositions in Table 3.1 were repeated again with quartz substrates. The sputtering parameters and conditions were described in Table 3.2. The thickness values for all the films were obtained from FILMETRICS 2000 optical reflectance thickness measurement tool.

Table 3.1: Deposition conditions of ZrO_2 films deposited at various substrate temperatures. Types of substrates used were glass and silicon

S. No	Sample Name	Ar flow (sccm)	RF power (W)	Substrate temperature (^oC)	Deposition duration in (min)	Pressure (m Torr)	Thickness (nm)
1	ZrGWO7	50	80	400	30	2.8	143
2	ZrGWO6	50	80	300	30	2.8	149
3	ZrGWO5	50	80	200	30	2.8	149
4	ZrGWO4	50	80	RT	30	2.8	154
5	ZrGWO8	50	80	100	30	2.8	152

Table 3.2: Deposition conditions of ZrO_2 films deposited at various substrate temperatures. The type of substrates used was quartz.

S. No	Sample Name	Ar flow (sccm)	RF power (W)	Substrate temperature (^oC)	Deposition Time (min)	Pressure (m Torr)	Thickness (nm)
1	ZrGWQO10	50	80	400	20	2.8	79.4
2	ZrGWQO9	50	80	300	20	2.8	80.2
3	ZrGWQO8	50	80	200	20	2.8	80.4
4	ZrGWQO7	50	80	100	20	2.8	80.2
5	ZrGWQO6	50	80	RT	20	2.8	81.4

RT = Room temperature (~ 30 ^oC)

3.3 Characterization

The samples grown at varying substrate temperatures were characterized using advanced analytical methods such as HRSEM, HRTEM and Grazing Incidence X-ray Diffraction (GIXRD), X-ray reflectivity (XRR), and optical spectrophotometry.

3.3.1 Surface morphology

Hitachi S-4800 high resolution scanning electron microscopy was used to observe surface morphology. This SEM has magnification capability of x800K and can achieve high resolution micrographs for a magnification of x300k. All the ZrO_2 films deposited on Si are analyzed and high resolution micrographs of film surfaces were obtained and microstructure of the films was quantified.

3.3.2 ZrO_2/Si cross section analysis

ZrO_2 reacts with silicon and forms an interface layer of Zr-O-Si alloy when deposited on silicon. HRSEM and HR-TEM techniques were used to analyze and quantify the interface layer. Sample ZrGWO7 was analyzed with HRTEM because it is assumed that interface layer will be ultra thin for this sample, so it cannot be seen on HRSEM.

3.3.2.1 TEM analysis

UTEP collaborated with Microelectronics research center, UT Austin for cross-sectional TEM analysis for selected samples. FEI TECNAI G2 F20 X-TWIN Transmission Electron Microscope (TEM) is an analytical system with excellent high-resolution imaging and atomic resolution microanalysis capabilities. The system is optimized for high spatial resolution analysis. Cross-sectional samples for transmission electron microscopy analysis (TEM) are prepared by using a dual beam System (FIB/SEM) FEI Strata 235, employing 30 kV Ga + ions, with a final beam current of ~50 pA. Samples were then plasma cleaned for 7 minutes in a South Bay Technology PC200 system on a Ar/O_2 ambient and

subsequently characterized on a schottky field-emitter based FEI Tecnai TF20 (200kV) equipped with a STEM unit, high-angle annular dark-field (HAADF) detector and X-Twin lenses. The specimen observation was carried out with the sample aligned to the nearest <110> zone axis of the silicon substrate.

3.3.3 Structural characterization

Structural characterization involves investigating crystal structure of the film. Determining the preferred crystallographic orientation (if any), crystal quality information, crystal structure, and crystallite size is of particular importance. XRD is an analytical technique in which x-ray beam hits the surface of a substrate at various incident angles scattering preferentially oriented x-rays into detector which collects them to generate crystallographic information about the sample such as lattice parameter, d-spacing, film orientation. XRD principle is based on Bragg's law

$$\lambda = 2dsin\theta$$

where λ = wave length of x- rays

d = inter planar distance

and θ = Bragg's angle,

However, ordinary x-ray diffraction does not work for thin films because of the small volume of the material and the domination of substrate background. For thin films, therefore, grazing incidence XRD (GIXRD) will be used. In GIXRD a parallel, monochromatic x-ray beam is incident on the sample surface at a fixed angle of incidence and the diffraction profile is recorded by a detector only scan.

ZrO_2 samples were analyzed with GIXRD and XRR techniques. GIXRD scans were first run at incident angles of 0.5^o, 0.3^o and 0.1^o with detector scan step size of 0.06^o. Then comparison of samples grown at various T_s has been made using the measurements at an incident angle of 0.5^o, where the information from the film alone can be best obtained as seen in this work.

3.3.4 Optical spectrophotometry

Optical spectrophotometry is another simple and versatile analytical technique for optically transparent and semi-transparent thin films. Usually, the films deposited on optically transparent substrate such as glass, quartz, sapphire substrates will be employed for such measurements. Using spectrophotometry (transmission and reflectivity), n (refractive index), k (extinction coefficient), dielectric constant and band gap of the thin film materials can be calculated.

Optical band gap of ZrO_2 thin films was calculated by optical transmission measurements made using Cary 5000 UV-Vis- NIR dual beam optical spectrophotometer. Transmission measurements were made on ZrO_2 films deposited (depositions conditions are described in Table 3.2) on quartz substrates over a wide range i.e., 185 nm – 2000 nm. The light beam is continuous and has 1 nm resolution.

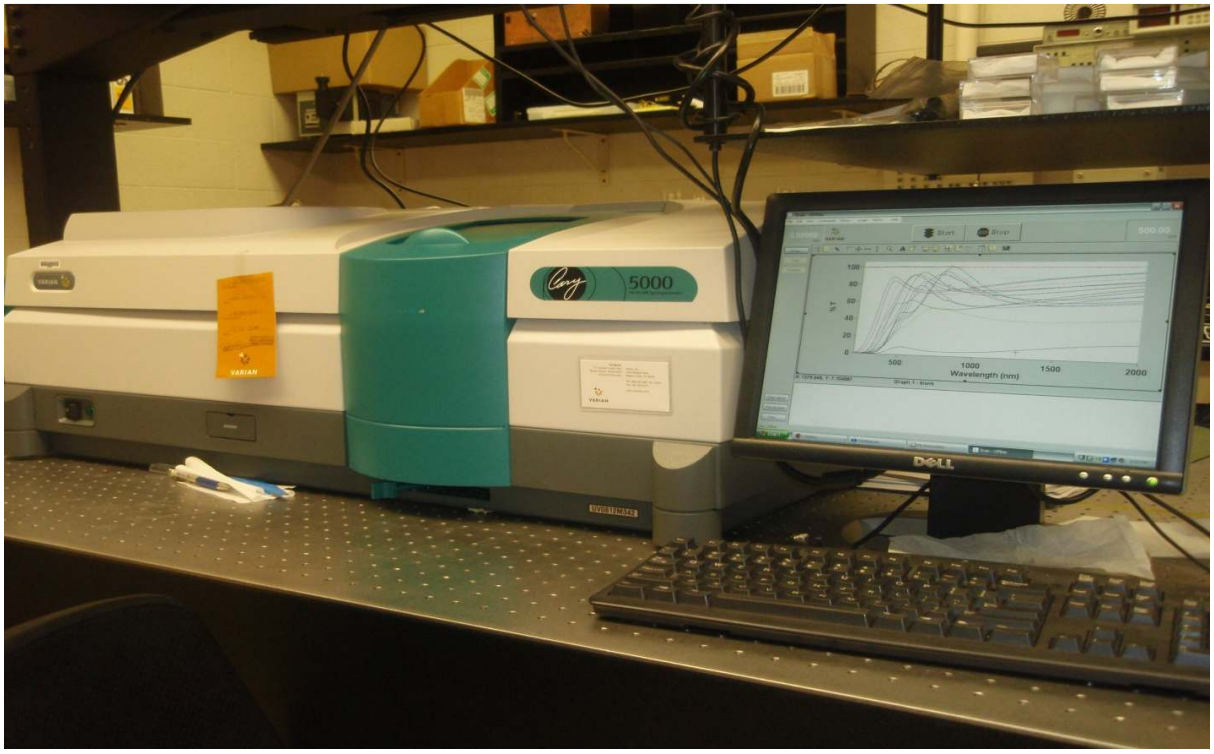

Figure 3.2: Cary 5000 UV - Vis - NIR spectrophotometer

3.4 MOS devices

The Metal – Oxide – Semiconductor (MOS) capacitive structures were built to emulate dielectric stack in MOSFET and C-V curves were obtained to validate the performance of ZrO_2 as gate dielectric. ZrO_2 films were deposited at room temperature and annealed at 400 ^{0}C to investigate the effect of annealing temperature on microstructure and films morphology, interface layer and electrical properties of the ZrO_2 films. The fabrication of MOS structures involves following steps.

- Deposition of Aluminum metal on to Silicon wafer back surface create back electrode contact
- Deposition of ZrO_2 on surface of Si
- Annealing (for select samples)
- Deposition of selective area top electrode contact deposition.

3.4.1 Fabrication

3.4.1.1 Back electrode contact deposition

Aluminum (Al) was deposited on to back surface of silicon substrate, using thermal evaporation method. KJLC deposition system was equipped with RGA industries thermal evaporation power supply and electrode system. A tungsten (W) basket filled with Al pellets was placed between thermal evaporation power supply electrodes. The vacuum chamber was pumped down to $7x10^{-7}$ Torr. A DC voltage of 100 V was applied and DC current was increased from 0-20 Å. The DC power applied across heats tungsten basket and evaporates Al. The evaporated Al will be deposited onto Si substrates placed above the thermal evaporation system. In these experiments, 700-800 nm thick Al film was deposited onto each Si substrate. Aluminum deposited onto silicon forms metal – semiconductor schottky junction, which interferes with electrical properties of MOS structure. To make this back contact an ohmic

contact, the aluminum films are in situ vacuum annealed at 450 ^{o}C for 30 min using halogen heater lamps inside the deposition chamber.

3.4.1.2 Deposition of ZrO_2 gate dielectric

ZrO_2 films are direct sputter deposited using a pure ZrO_2 target on back contacted Si substrates. A sputter power of 80 W is applied to the target at 2.8 mTorr of Ar pressure for 10 mins. The sample was segregated into two parts, one part (ZrOAC1.1) was further proceeded to annealing and top contact metallization and other part was (ZrOAC1.2) directly proceeded to direct top contact metallization without anneal.

Table 3.3 depicts the deposition conditions of substrates fabricated for MOS structure.

Table 3.3: Deposition conditions of ZrO_2 films for MOS structure fabrication.

S.No	Sample name	Ar flow in sccm	RF power in watts	Substrate temp. in ^{o}C	Deposition duration in min	Types of substrates	Thickness in nm
1	ZrOAC1	50	80	RT	10	Si	42

Table 3.4: Annealed and not annealed samples

Anneal	No anneal
ZrOAC1.1	ZrOAC1.2

3.4.1.3 Annealing

Post deposition annealing was performed on the oxide films in THERMTEC three zone quartz tube furnaces. Figure 3.5 shows the THERMTEC three zone furnace. The annealing was performed at 450 ^{o}C for 15 min in forming gas (3.5 % -5 % H_2 + 95 % N_2) ambient. The forming gas ambient

introduces reducing environment and removes dangling bond and point defects in the oxide film. The substrates intended to anneal were introduced into the furnace purged with nitrogen for 5 min. The temperature was ramped up to 440 ^{o}C while substrates dwell in nitrogen ambient.

The nitrogen flow rate was 40sccm. After the temperature was ramped to 440 ^{o}C in 11 minutes, forming gas with flow rate 80 sccm was introduced into furnace tube and substrates were annealed for 15 min.

Figure 3.3: TERMTEC three zone furnaces

After this step the furnace was turned off and allowed to cool down to 65 ^{o}C. Throughout the cooling cycle, N_2 at 40 sccm was blown into the furnace to provide inert ambient for substrates inside the furnace. The annealing cycle is illustrated in the Figure.3.4

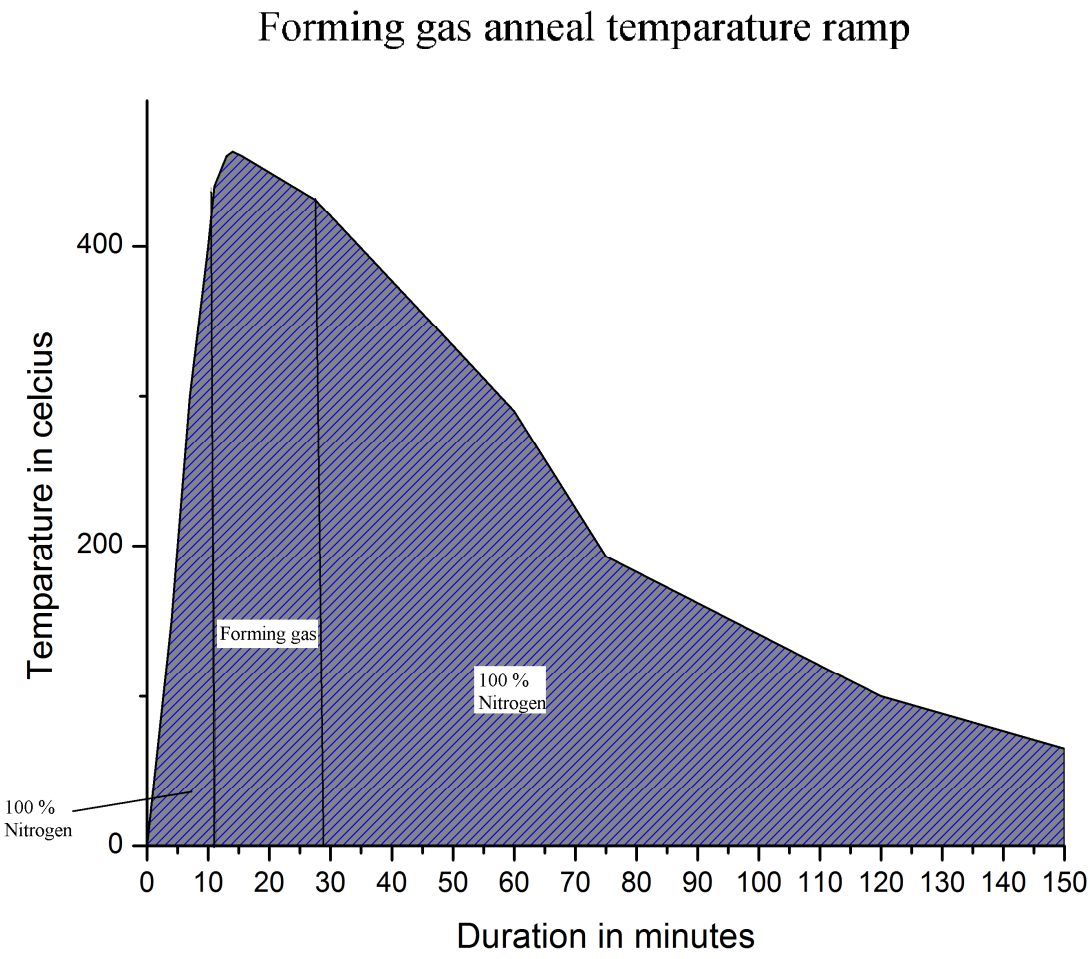

Figure 3.4: Forming gas anneal temperature curve

3.4.1.4 Top contact metallization

Small circles of the top Al metal contacts were formed on samples ZrOAC1.1 and ZrOAC1.2, using thermal evaporation method using stainless steel mask. 500 nm of Al contacts were deposited onto the ZrO_2 films. This step concludes the fabrication of MOS structure. The cross section view of MOS structure thus formed is illustrated in Figure 3.5

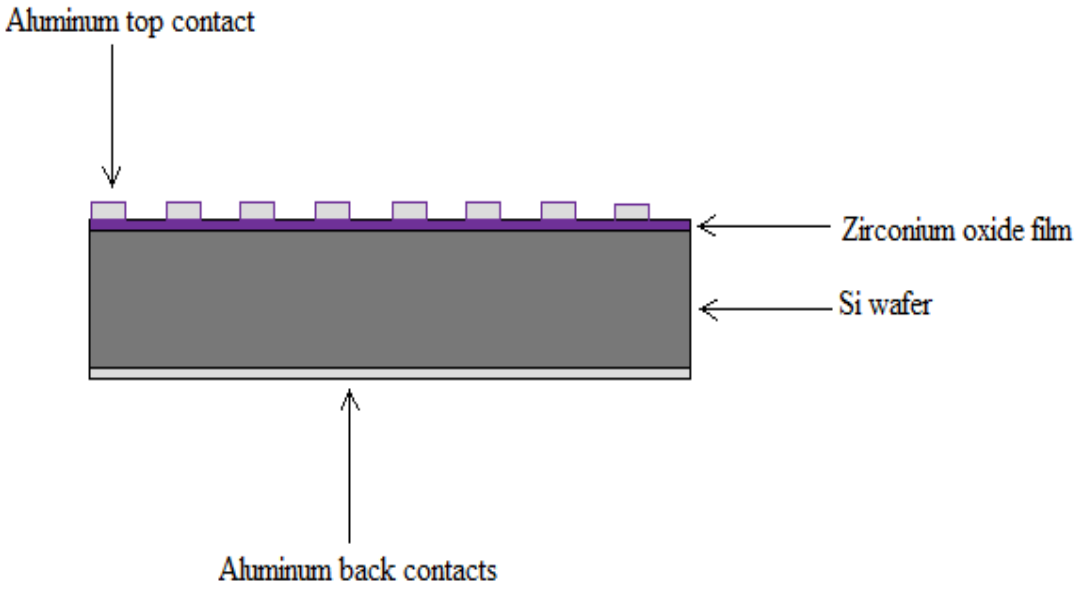

Figure 3.5: Al/ ZrO_2/Si/Al MOS structure

3.4.2 C – V curves

The C–V curves for MOS capacitors (ZrOAC1.1 and ZrOAC1.2) were obtained with a Boonton 7200 capacitance meter. The apparatus for C-V curves is as shown in Figure 3.6. The capacitance meter is capable of measuring a voltage of 2000 pF. The Capacitance meter's Hi terminal was connected to the top metal contact and Lo was connected to the Al back contact. The Voltage was swept between -25 – 20 V.

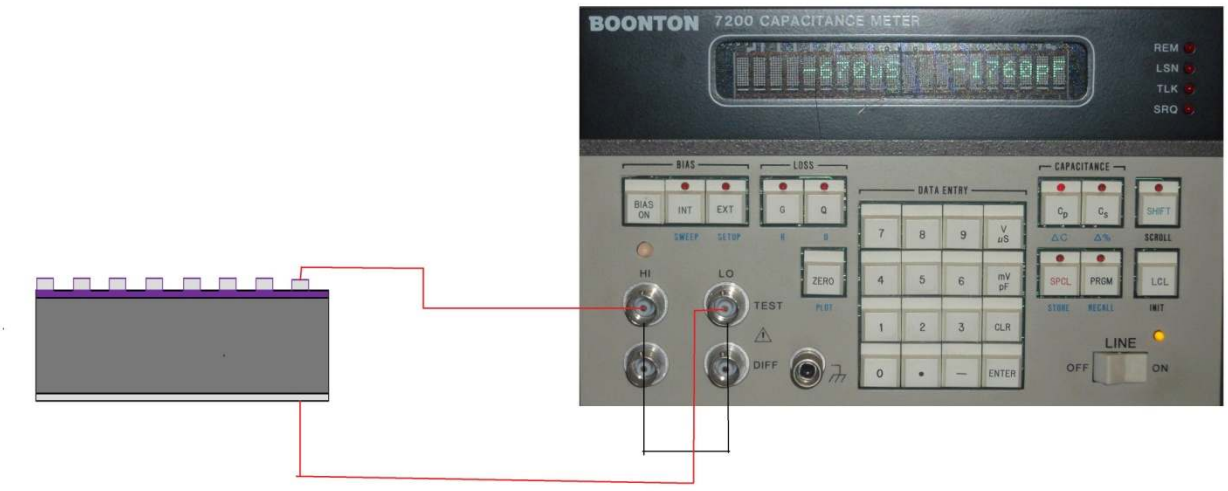

Figure 3.6: C- V measurement setup

Chapter 4: Results and Discussions

4.1 Characterization

ZrO_2 films were deposited (as described in Table 3.1) to study their surface morphology, interface structure and composition, crystal structure, optical and electric properties as a function of growth temperature. Various experimental and analytical techniques and instruments were used for these investigations. A brief summary of the tasks that are most important or targeted aspect of ZrO_2 films is listed below along with the main technique employed. This list provides a general outlook of the overall efforts made in this work.

Film thickness	-	Film metrics 2000 optical reflectance thickness measurements
Surface morphology	-	High resolution scanning electron microscope
ZrO_2 /Si interface analysis	-	High resolution transmission electron microscope (HRTEM), X- Ray reflectivity (XRR)
Crystal structure	-	Grazing incidence x-ray diffraction (GIXRD)
Optical properties	-	UV - Vis - NIR double beam spectrophotometer
Electrical properties	-	Capacitance-voltage (C-V) measurements

4.2 Surface morphology

It is important to derive information on surface quality, grain size and particle distribution characteristics are important factors govern the film quality and properties. The surface morphology of films grown at various T_s (ZrGWO4, ZrGWO5, ZrGWO6, and ZrGWO7) are shown in Figures 4.1 – 4.4

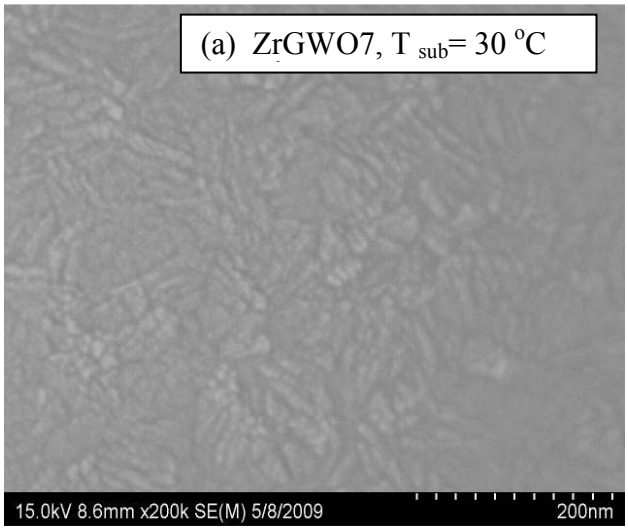

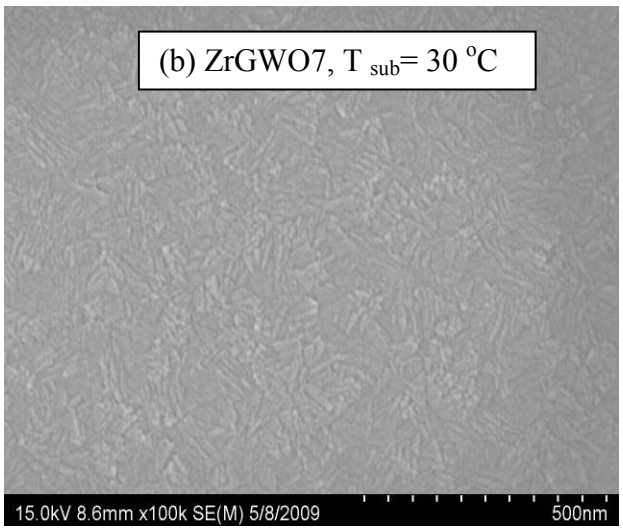

Figure 4.1: SEM micrograph of ZrO_2 deposited at substrate temperature of RT (~30 ^oC) (a) Low magnification, (b) Low magnification

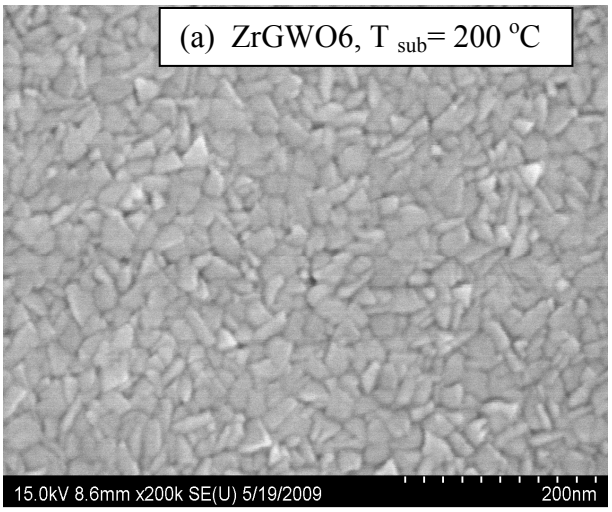

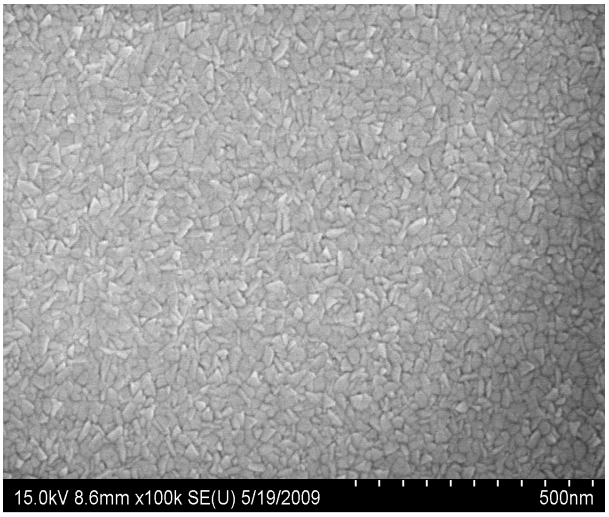

Figure 4.2: SEM micrograph of ZrO_2 deposited at substrate temperature of 200 ^0C (a) Low magnification, (b) High magnification,

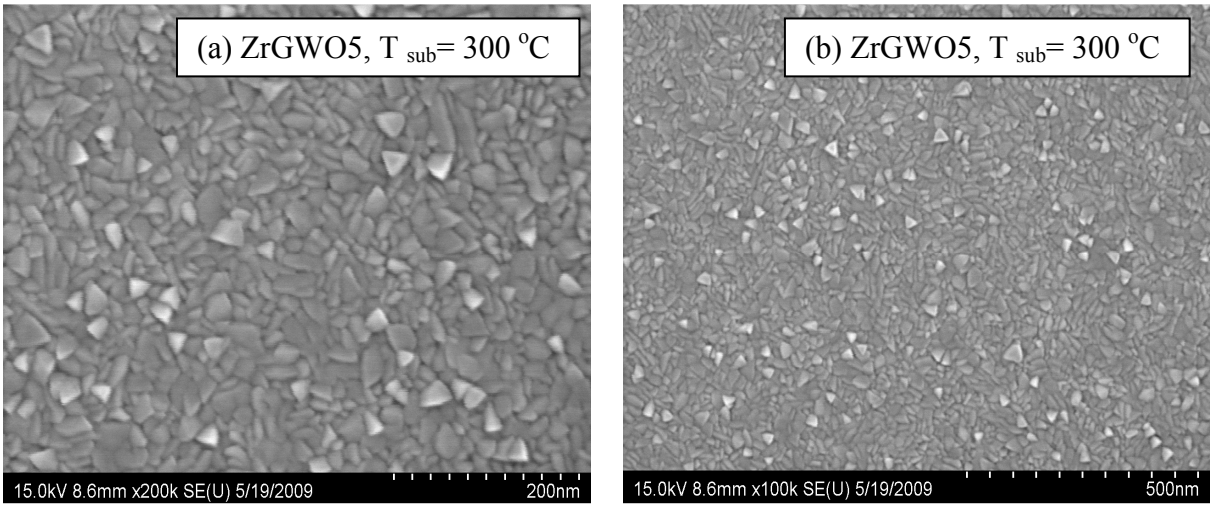

Figure 4.3: SEM micrograph of ZrO_2 deposited at substrate temperature of 300 ^{0}C (a) High magnification, (b) Low magnification,

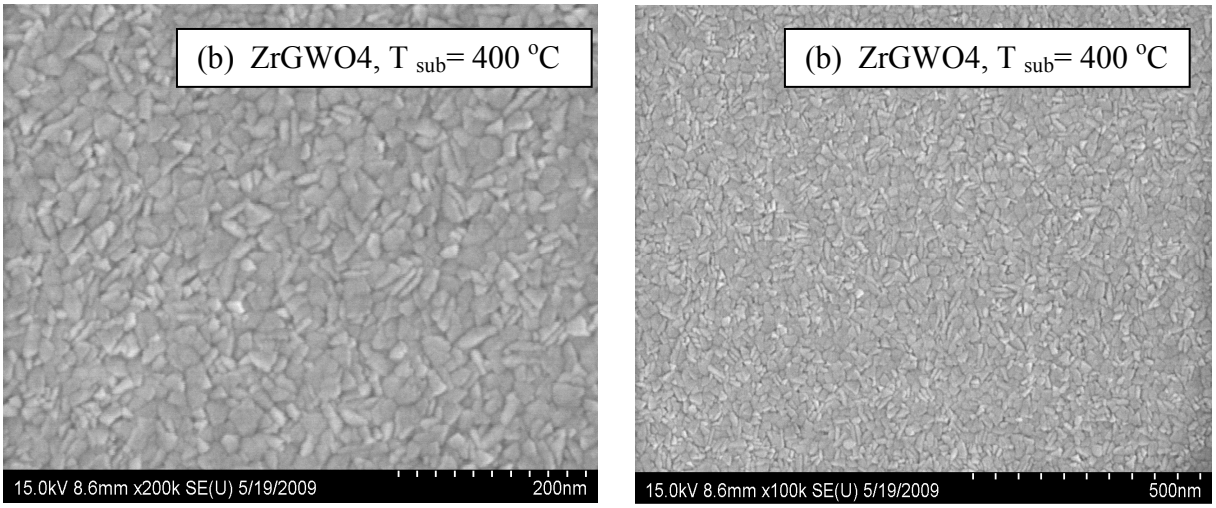

Figure 4.4: SEM micrograph of ZrO_2 deposited at substrate temperature of 400 ^{0}C (a) High magnification, (b) Low magnification,

It can be seen in the SEM micrographs (Figure 4.1(a) and (b)) the surface of ZrO_2 grown at room temperature exhibits smooth surface texture. To the limit of HRSEM the surface of the sample looks only partially crystallized while most of the part is amorphous. However, the XRD results discussed later indicates that the films are nanocrystalline and oriented. SEM micrographs of the sample

grown at substrate temperature of 200 ^{o}C (Figure 4.2(a) and (b)) indicates changes in the morphology, compared to samples grown at room temperature. These samples exhibit morphology where the fully crystallized state of ZrO_2 is evident. The crystallite size is ~20 nm. Further increase in temperature increases the grain size and favors the formation of faceted crystals (Figures 4.3(a) and (b)). Compared to samples grown at 300 ^{o}C and 400 ^{o}C there is a clear change in surface morphology as the grain sizes and shapes are different. The grains in sample grown at 300 ^{o}C are faceted and are little smaller than the grains in sample grown at 400 ^{o}C. The grain sizes were measured by calibrating the images with QUARTZ PCI software. The smallest grain size was found to be ~5nm and the largest grain size measured is 40 nm. The average grains sizes were measured by counting number of grains against a calibrated scale on the SEM micrograph. The average grain sizes were 12 nm, 15 nm and 20 nm for samples deposited at 200 ^{o}C, 300 ^{o}C and 400 ^{o}C respectively.

This research work strives to validate ZrO_2 films as high–κ dielectric. One of the most stringent surface morphology requirements of high–κ dielectric oxide is that film should be amorphous or nano-crystalline and should be dense. From HRSEM investigations of the surface morphology, it is obvious that the grown ZrO_2 films are dense. However, the grain size increases with substrate temperatures.

Upon comparing the surface morphologies of all the samples, the size and shape of the grains found to be entirely different. This behavior can be attributed to interface layer formation at ZrO_2/Si interface. The interface layer is a Zr–Si–O ternary system and there is a possibility of forming $ZrSi_x$ or $ZrSi_xO_y$ or SiO_2 depending on surface energetic and free energy change (ΔG). The chemical composition of interface and surface energetics play an important role in grain formation mechanisms. Also there is a possibility of crystal structure change for different substrate temperatures which in turn changes the surface morphology.

4.3 Interface analysis

The thermodynamic information of ZrO_2/Si interface reveals that ZrO_2 reacts with Si either to form very thin layer of $ZrSi_x$ or SiO_2 or ZrO_x. The interface for room temperature grown ZrO_2 sample (ZrGWO7) was analyzed with cross sectional TEM and Scanning TEM–EDX. The HRTEM micrograph of the ZrO_2/Si cross-sectional structure is shown in Figure 4.6. The existence of an interfacial layer (IL) between the grown ZrO_2-film and Si-substrate is evident in the HRTEM image. The thickness of the sample is 145 nm and thickness of IL is 2.68 nm. The substrate, IL and film regions are indicated in Figure 45 along with the measured thickness values for film and IL.

The very-high magnification images obtained from HRTEM in the areas along with the ZrO_2 film region are shown in Figure 4.6. The regions used for obtaining the high-resolution magnification are shown with squares. Those obtained in the process are shown in right-hand panel. It can be seen that the images obtained exhibit the lattice-fringes, which corresponds to the crystallized zirconia.

The most important points derived from HRTEM are the following: (1) thickness of the grown zirconia film is ~145 nm, (2) 2.68 nm thick IL formation takes place; (3) local structure of the ZrO_2 film is crystallized. These observations indicate that the reaction between the Si substrate and growing ZrO_2 film readily takes place even without a high-temperature environment. However, the most noteworthy point of our investigations is that our approach limits IL thickness to 2.6 nm for a zirconia film of 145 nm thick. For instance, Chen et al. have reported a 7 nm thick IL formation when zirconia film was fabricated by reactive magnetron sputtering without premeditated substrate heating [22]. Furthermore, their IL value is for a relatively thinner zirconia film i.e., ~ 40 nm.

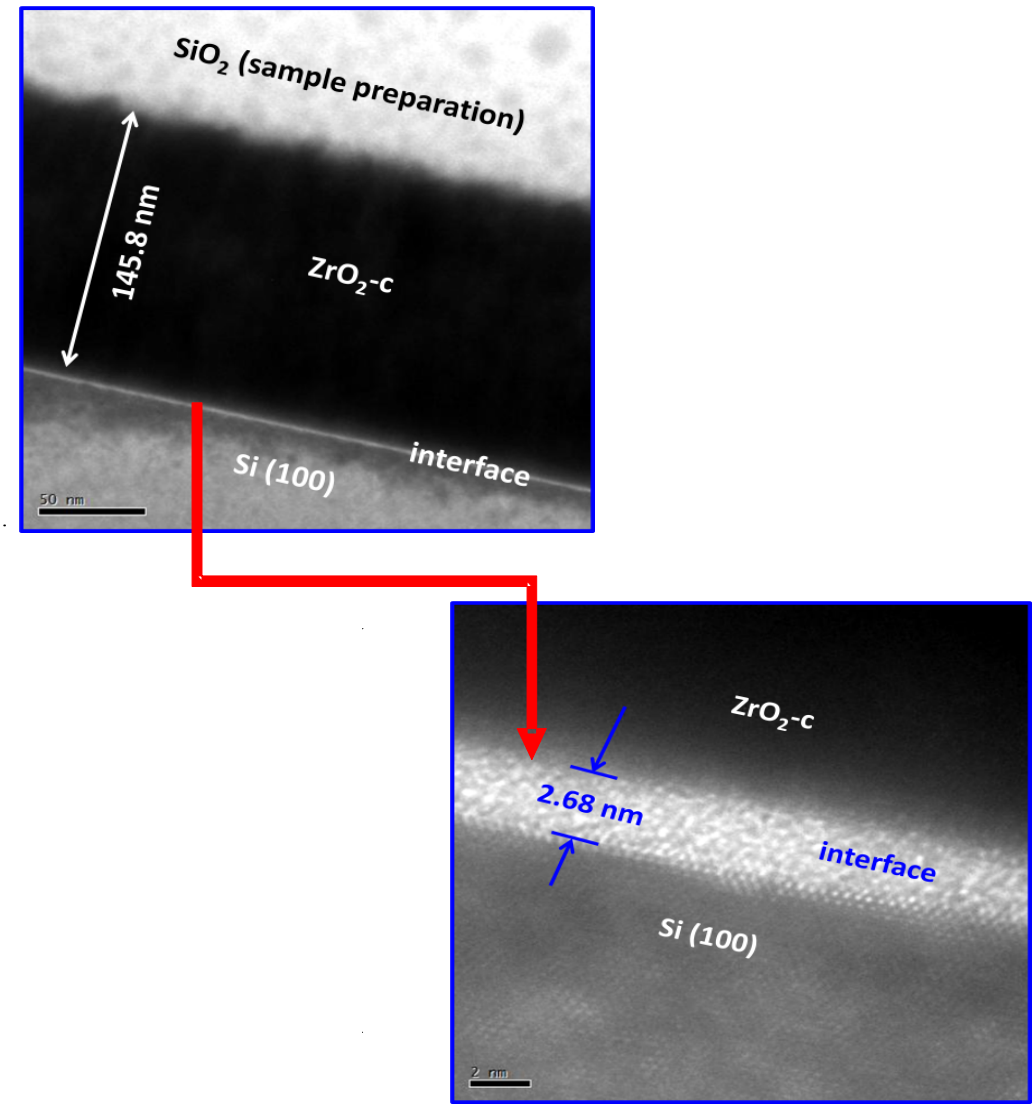

Figure 4.5: The Cross section TEM image of ZrO_2 (ZrGWO7, T_s=RT)

The interface layer is completely amorphous. The interface is a Zr-Si-O mixed phase system as seen STEM-EDX analysis. According to Schlom et al [7], the composition of interface could be ZrO_2 dominant or SiO_2, if there is no possibility of forming ternary phase such as Zr_xSiO_y. It is evident from STEM–EDX data (Figure 4.8), particularly rectangle boxed area of ZrO_2/Si interface, the interface is dominant with Zr and Si species.

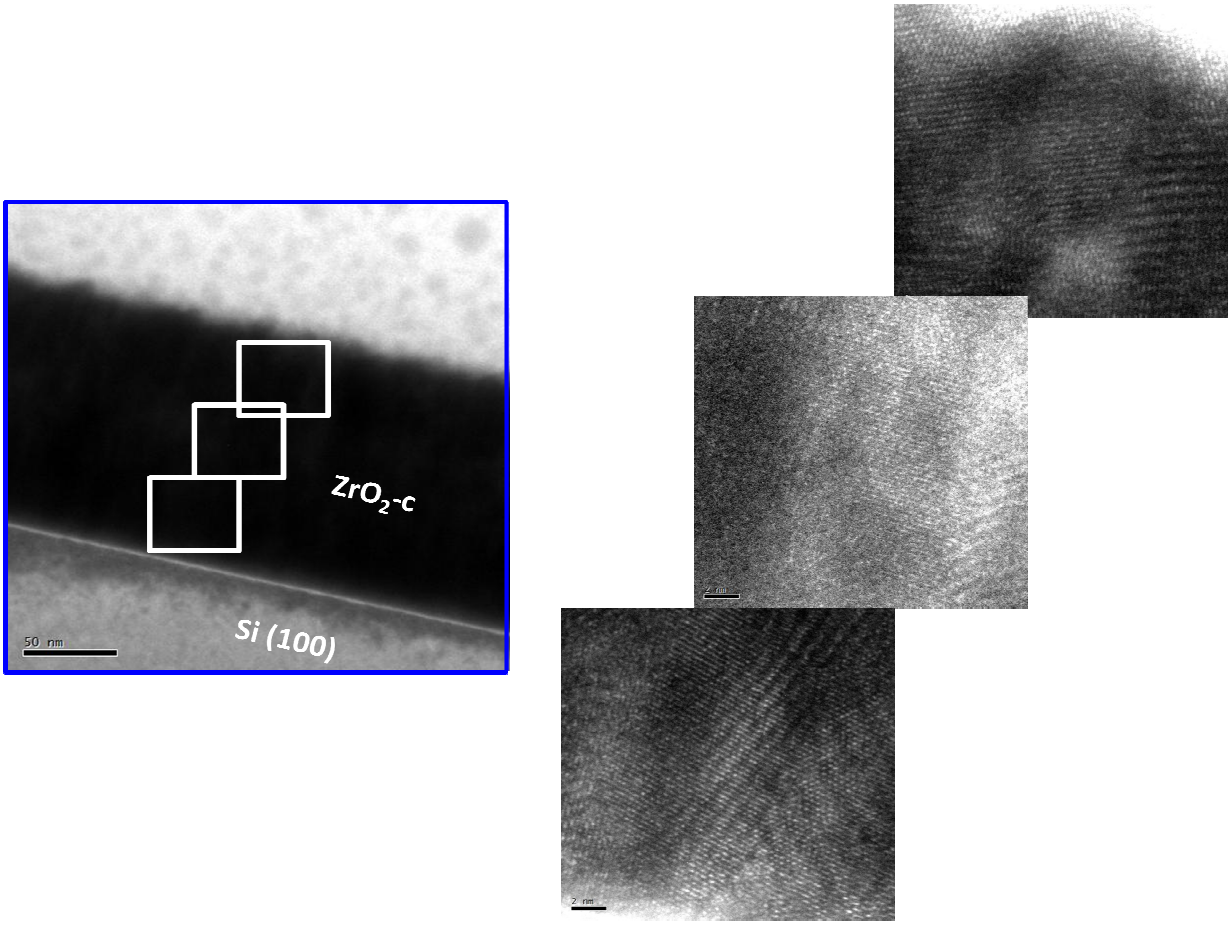

Figure 4.6: HRTEM image of ZrO_2 film deposited at RT

The STEM-EDX observation leads to the conclusion that the interface is actually a zirconium silicide $ZrSi_x$. The silicide formation is not desirable, because it is conductive and could compromise the performance of MOSFET. The interface layer can be minimized by surface thermal oxynitridation. Thermal oxynitridation is well established method in current CMOS technology [9] in which a thin layer of SiO_xN_y could be formed using thermal reaction of NO on Si surface. This oxynitride could act as a barrier layer which would stop interface layer formation.

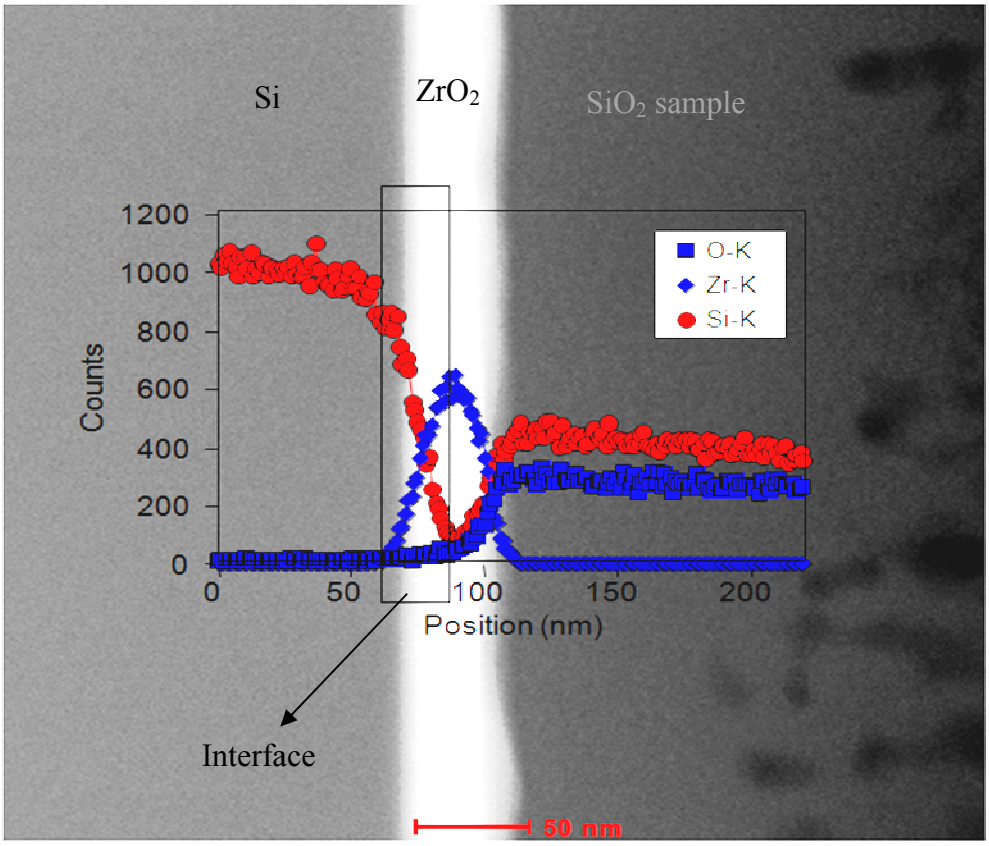

Figure 4.7: Scanning TEM EDX of ZrO_2 (T_s=RT)

4.4 Structural analysis

4.4.1 GIXRD

The ZrO_2 thin film samples grown were analyzed using GIXRD to understand the effect of T_s on crystal structure. The GIXRD spectra obtained at different grazing incidence angles are shown in Fig. 4.8 for ZrO_2 thin film grown at RT. The spectra reveal that the sample is nanocrystalline. Interestingly, the indexing of the pattern reveals that the films are crystallizing in cubic zirconia structure. Most of the peaks fit with the cubic-ZrO_2 as shown in Fig. 4.8.

The crystallite size is determined using the Scherrer's formula: $d=0.9\lambda/\beta\cos\theta$, where d is the size, λ is the wavelength of the filament used in the XRD machine, β is the width of a peak at half of its

intensity, and θ is the angle of the peak. The crystallite size determined from GIXRD is very small (~7 nm).

The GIXRD spectra of ZrO_2 films higher temperatures (200 ^oC and 300 ^oC) are presented in Figures 4.9 and 4.10. The curves are shown for various grazing incident angles. It is evident from the curves that all the films are nano-crystalline.

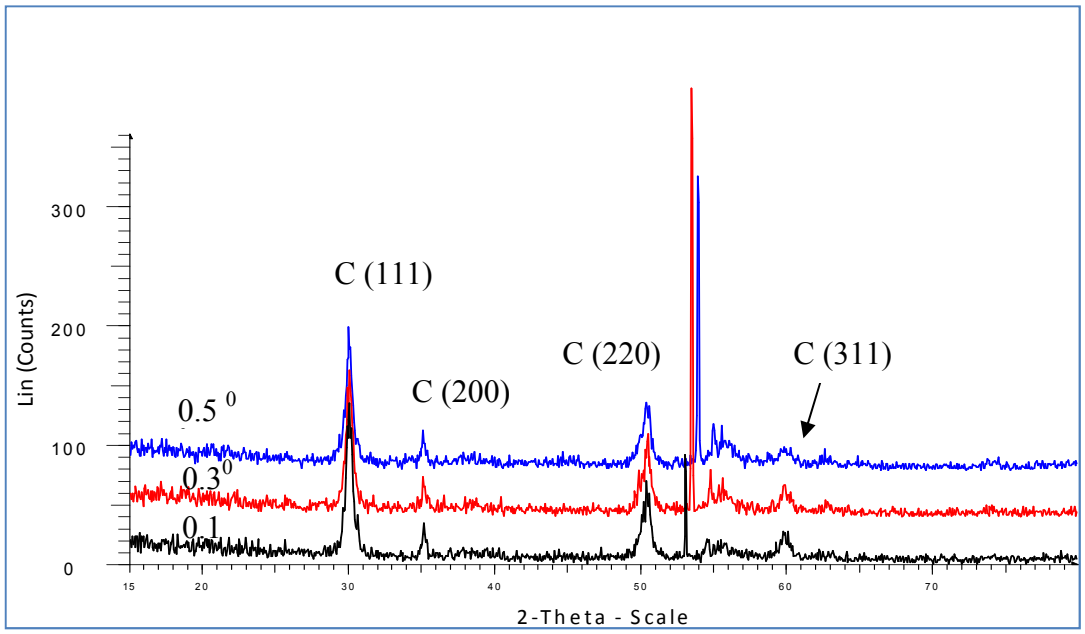

Figure 4.8: GIXRD spectra of ZrO_2 (T_s=RT, ID: ZrGWO7) at x-ray incidence angles of 0.5^0, 0.3^0, 0.1^0

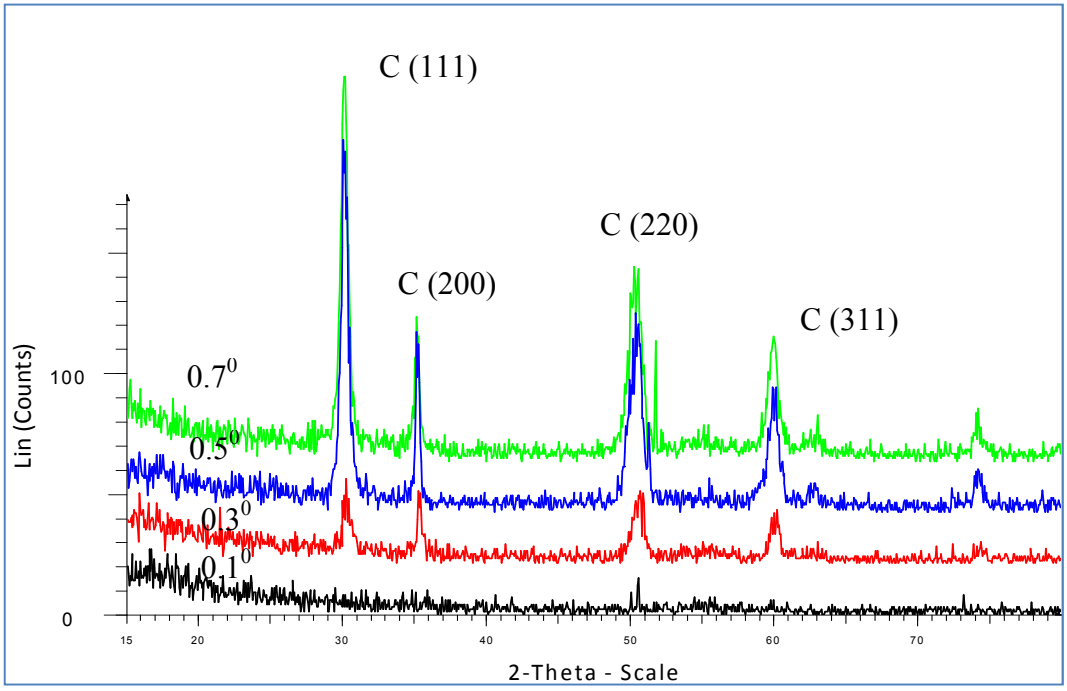

Figure 4.9: GIXRD spectra of ZrO_2 (T_s=200 ^oC, ID: ZrGWO6) at x-ray incidence angles of 0.5^o, 0.3^o, 0.1^o

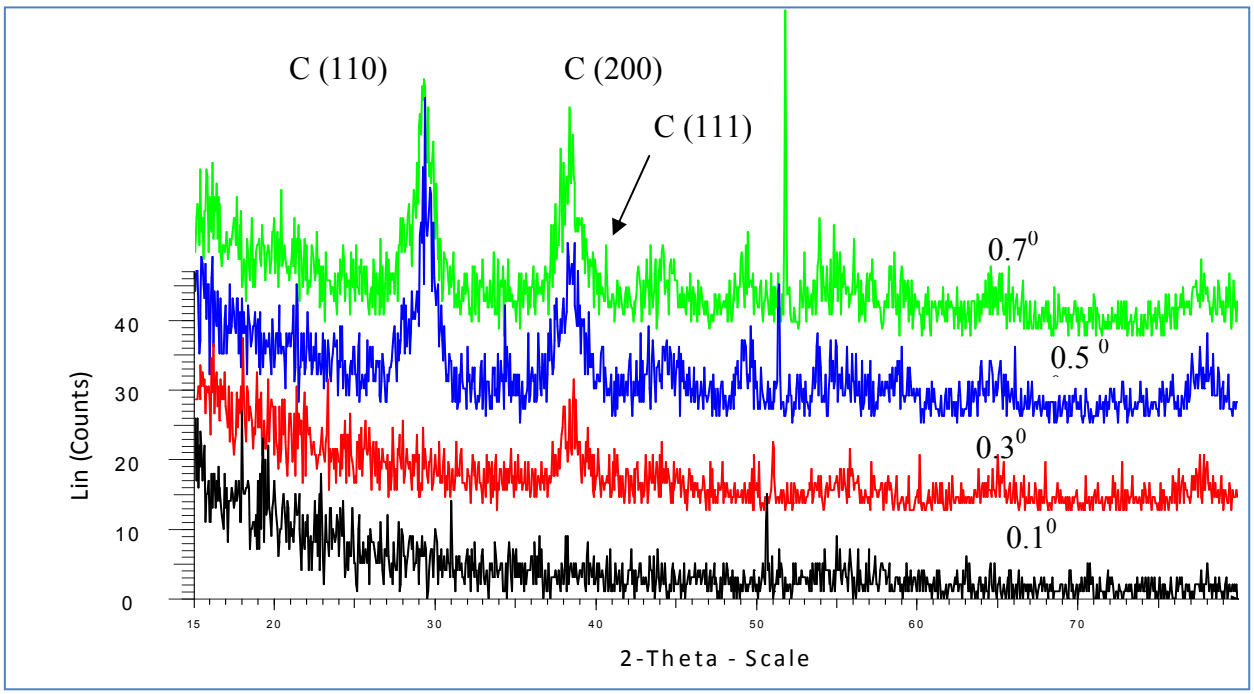

Figure 4.10: GIXRD spectra of ZrO_2 (T_s=300 ^oC, ID: ZrGWO5) at x-ray incidence angles of 0.5^o, 0.3^o, 0.1^o

A comparison of the GIXRD spectra obtained ZrO_2 films as a function of T_s is presented in Fig. 4.11. It is evident (Fig. 4.11) from the indexing of patterns that the films deposited at T_s=RT-200 ^oC exhibit the similar crystal structure. However, a structural transformation is noted at T_s=300 ^oC. The indexing of GIXRD pattern (Fig. 4.10) corresponds to a rutile phase instead of cubic phase. Figures 4.12 and 4.15 represent the simulated XRD spectra of cubic and rutile ZrO_2 phases, respectively. These models were built in CERIUS2® software using crystallographic information file [23-25] of open source crystal database. Upon comparing experimental and simulated XRD spectra, a solid conclusion is derived that the ZrO_2 films grown at T_s=RT-200^oC are cubic. A structural transformation from cubic-to-rutile occurs at 300 ^oC.

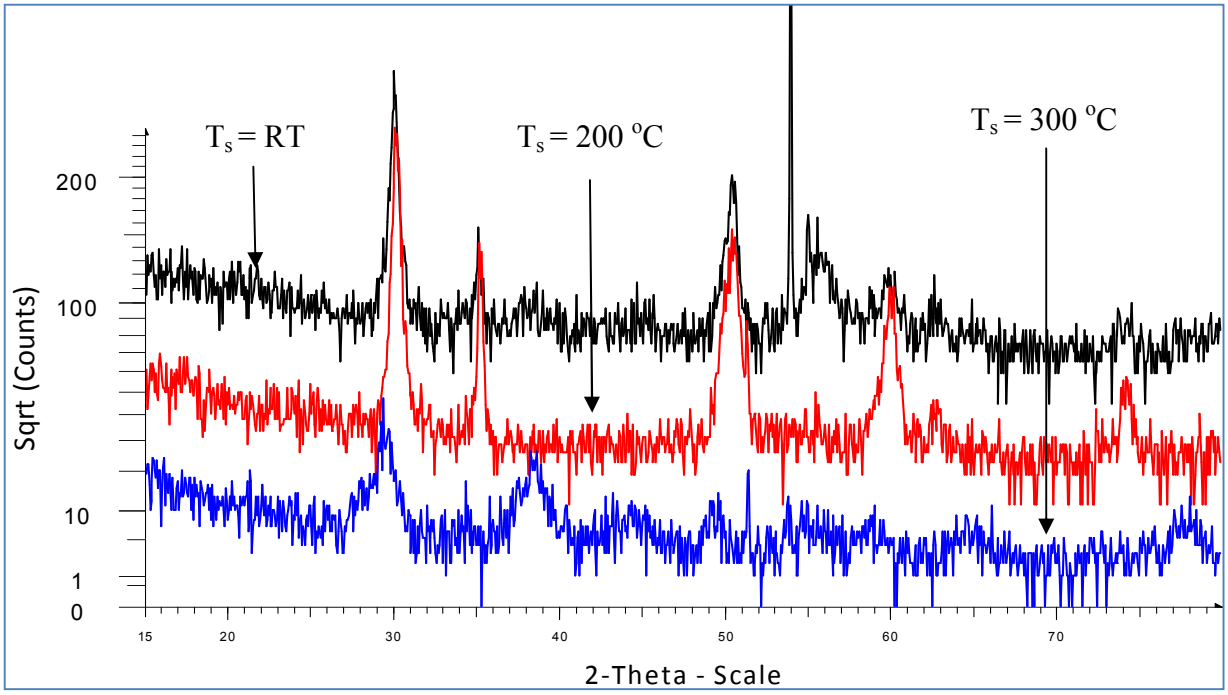

Figure 4.11: Comparison of GIXRD spectra of ZrO_2 grown at various T_s (ZrGWO5, ZrGWO6, ZrGWO7) at x-ray incidence angles of 0.5^o

The present GIXRD results and crystal formation can be understood if we consider the bulk of zirconia and its phases. ZrO_2, the thermodynamically stable phase in the Zr-O system, exhibits three

polymorphs: monoclinic (m-ZrO_2), tetragonal (t-ZrO_2), and cubic (c-ZrO_2) [26], at room temperature, m-ZrO_2 is the stable phase. It is reported that upon cooling from the melting point, ZrO_2 shows two kinds of solid–solid phase transformation, namely, cubic–tetragonal (c–t) [27], and tetragonal–monoclinic (t–m) [28-30]. The cubic-ZrO_2 is usually achieved only after sintering monoclinic or amorphous zirconia to high temperatures. Formation of the cubic phase in the present work can be attributed to the thermodynamics of crystal formation and stabilization at the nanoscale dimensions. The cubic phase of ZrO_2 has a fluorite structure, which consists of a fcc lattice of zirconium atoms eightfold coordinated to the neighboring oxygen atoms [Figure 4.14]. The zirconium site has the octahedral *Oh* symmetry, while the oxygen atoms are tetrahedrally coordinated to the zirconium atoms.

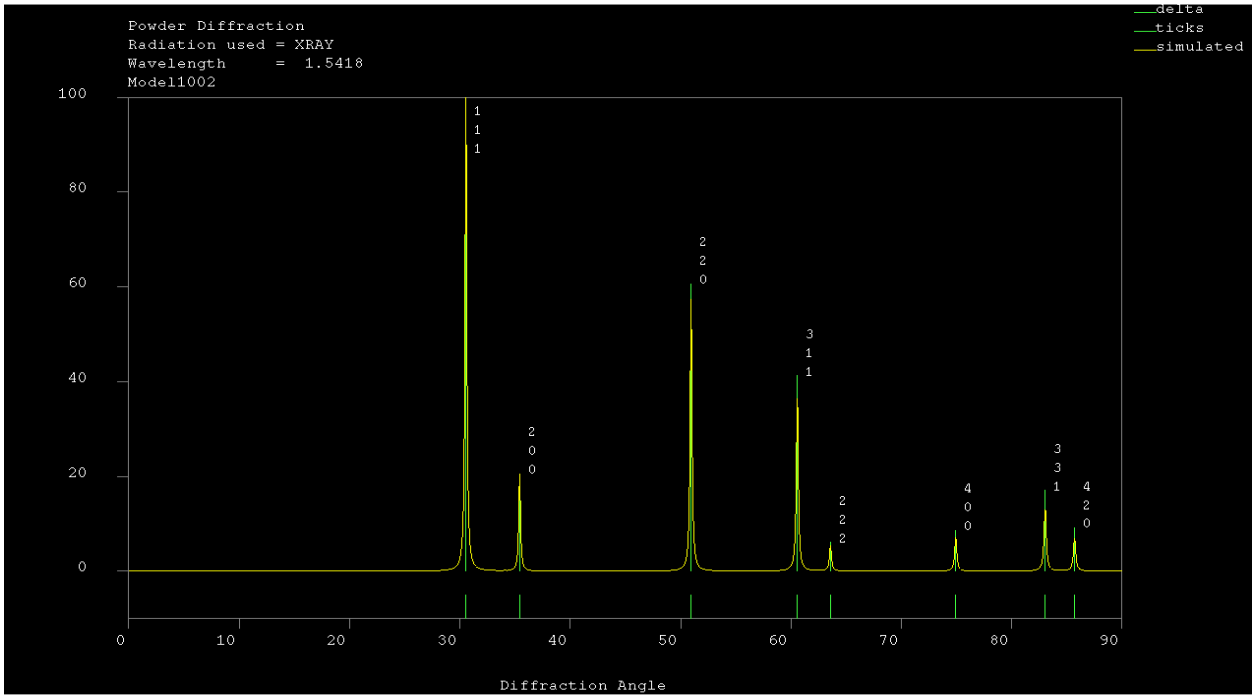

Figure 4.12: Simulated XRD spectrum of cubic ZrO_2

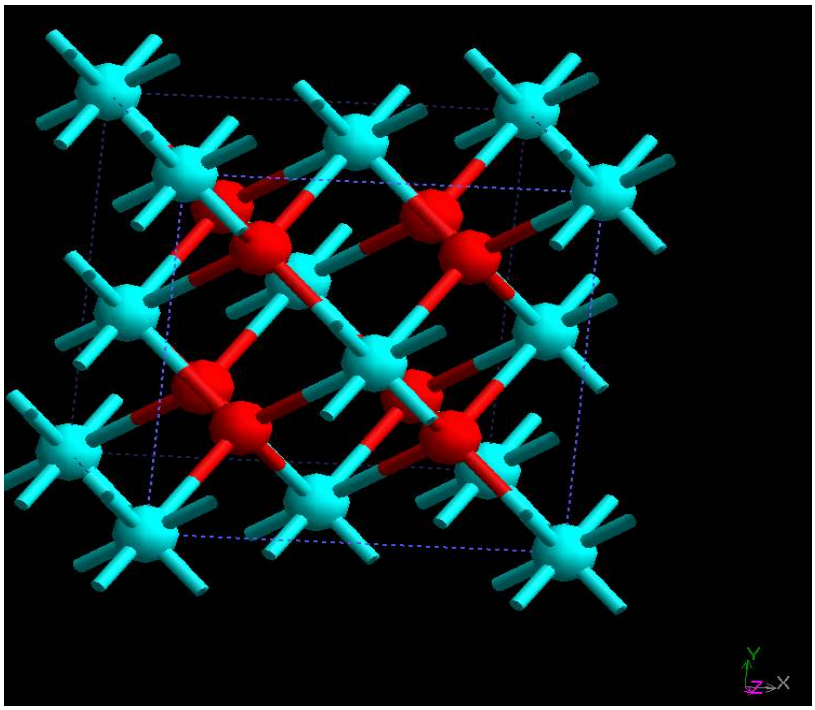

Figure 4.13: Crystal lattice of cubic - ZrO_2.

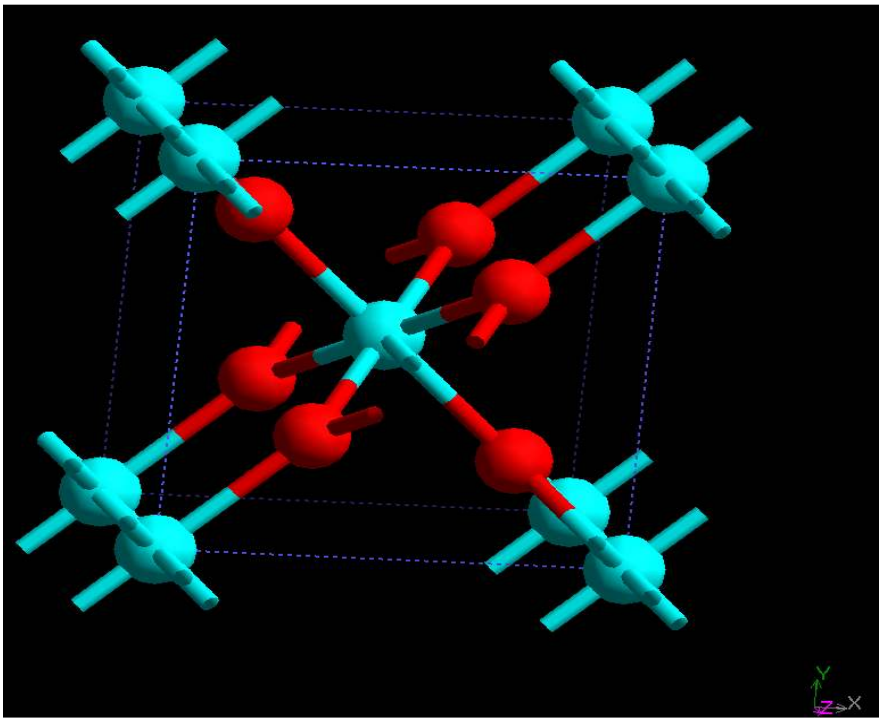

Figure 4.14: Crystal lattice of rutile-ZrO_2

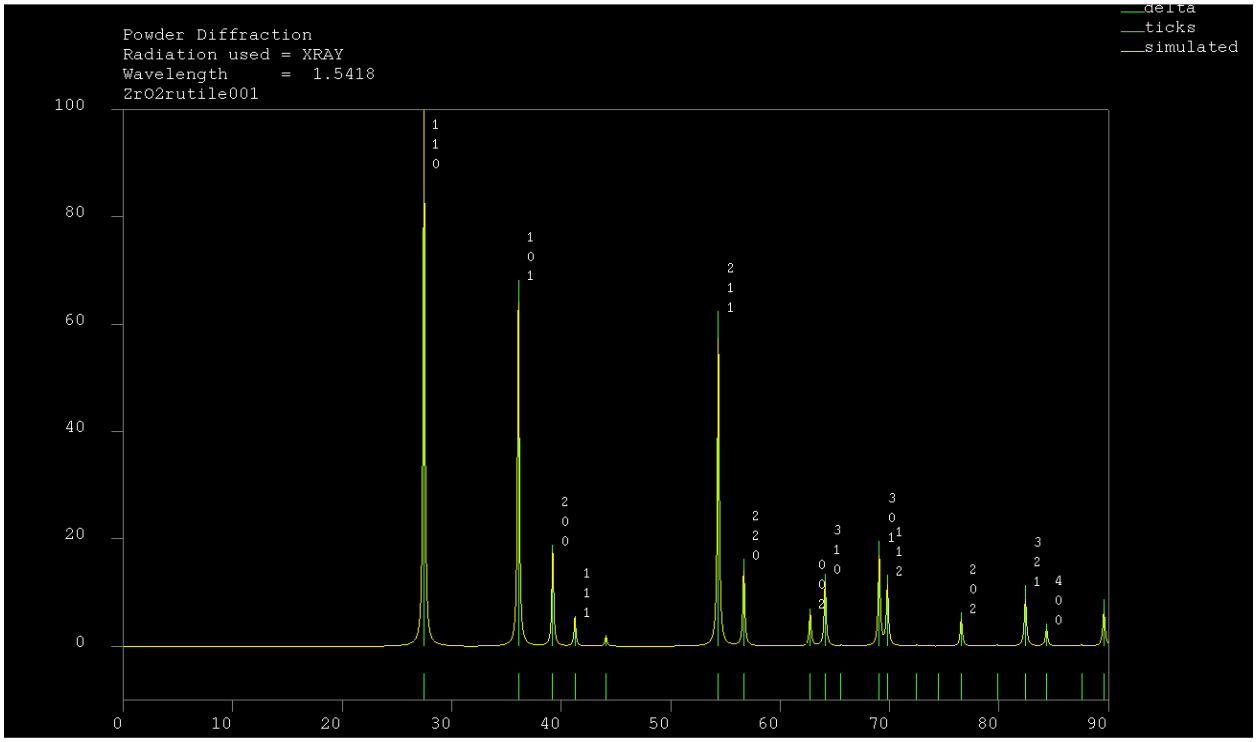

Figure 4.15: Simulated XRD spectrum of rutile ZrO_2

4.5 X- Ray reflectivity (XRR)

The x-ray reflectivity can give us the information about film thickness, film density and analysis of multi-layer films. XRR involves monitoring the x-ray beam reflected by a sample at grazing incidences. The XRR spectra of zirconia films are shown in Figure 4.16. The XRR data indicates the critical edge (Fig. 4.16; left-arrow red in color), which indicates that the surface layer density for all the films is consistent with that of ZrO_2. No interference pattern is observed for films grown RT-200 ^oC. This is due to the fact that the film is relatively thick and rough. However, for films grown at 300 ^oC, the interference pattern is a constructive superimposition of two interference patterns; one is film and the other is interface layer at the ZrO_2-Si interface.

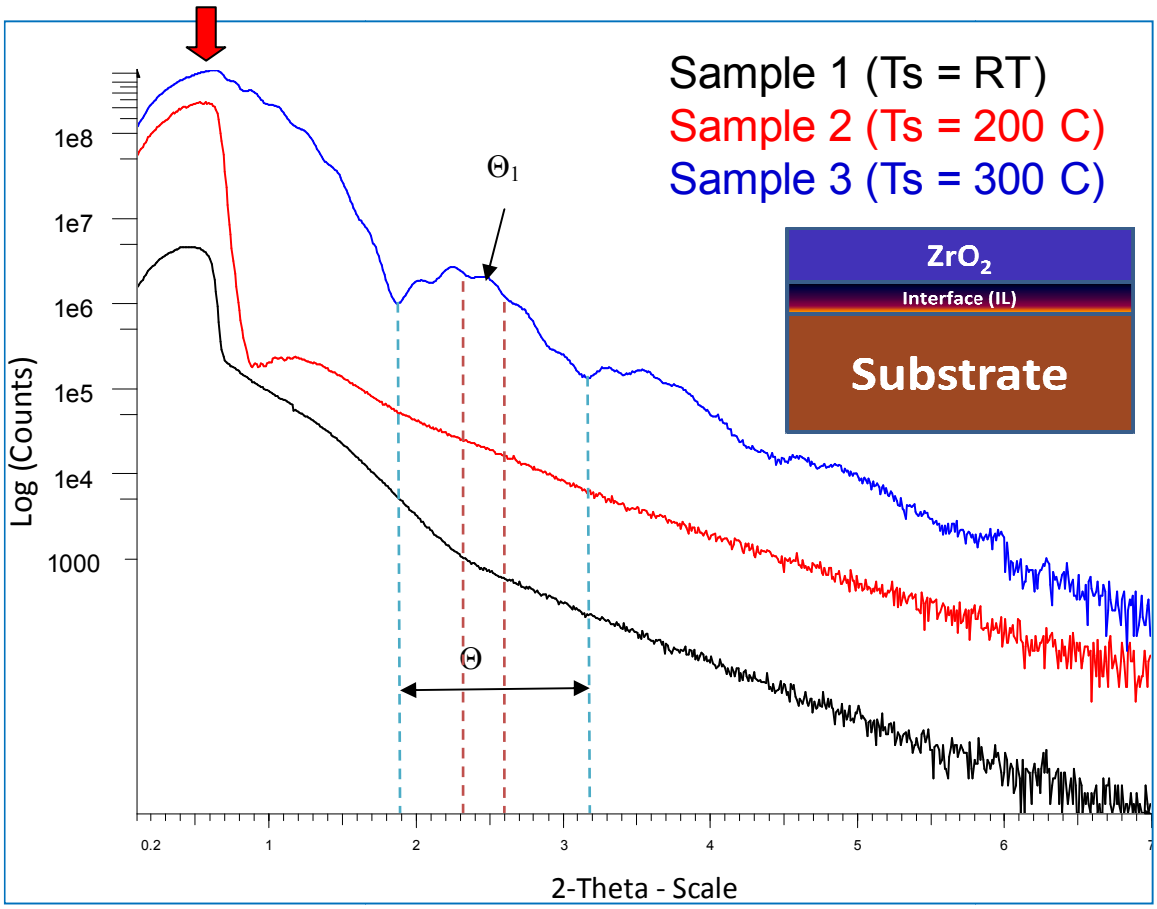

Figure 4.16: XRR spectra of ZrO_2 films grown at various T_s. Θ corresponds to interference of interface and Θ_1 corresponds to interference of ZrO_2 film. Insert shows the two-layer model evidenced in the XRR data for ZrO_2 films grown at $T_s \geq 300\ ^oC$.

The XRR data clearly indicates that the films grown at higher substrate temperatures ($T_s \geq 300\ ^oC$) will have the interface layers grow and account for reasonable thickness to show significant difference in the XRR pattern. The two-layer model containing the oxide-film and interface layer responsible for the observed results is shown in Fig. 4.16 as an insert.

4.6 Optical spectroscopy

The optical spectrophotometery is useful in determining the band gap, refractive index and extinction coefficient of transparent or semi transparent thin films. Figure 4.17 shows the UV-Vis-NIR spectral transmittance of ZrO_2 thin films deposited at various T_s. ZrO_2 thin films grown on quartz

substrates were employed for these measurements. It can be seen that ZrO_2 films exhibit a high optical transparency in the spectral region except where the incident radiation is absorbed across the fundamental absorption band edge. Such a behavior is characteristic of the ZrO_2 thin films with almost zero absorption losses.

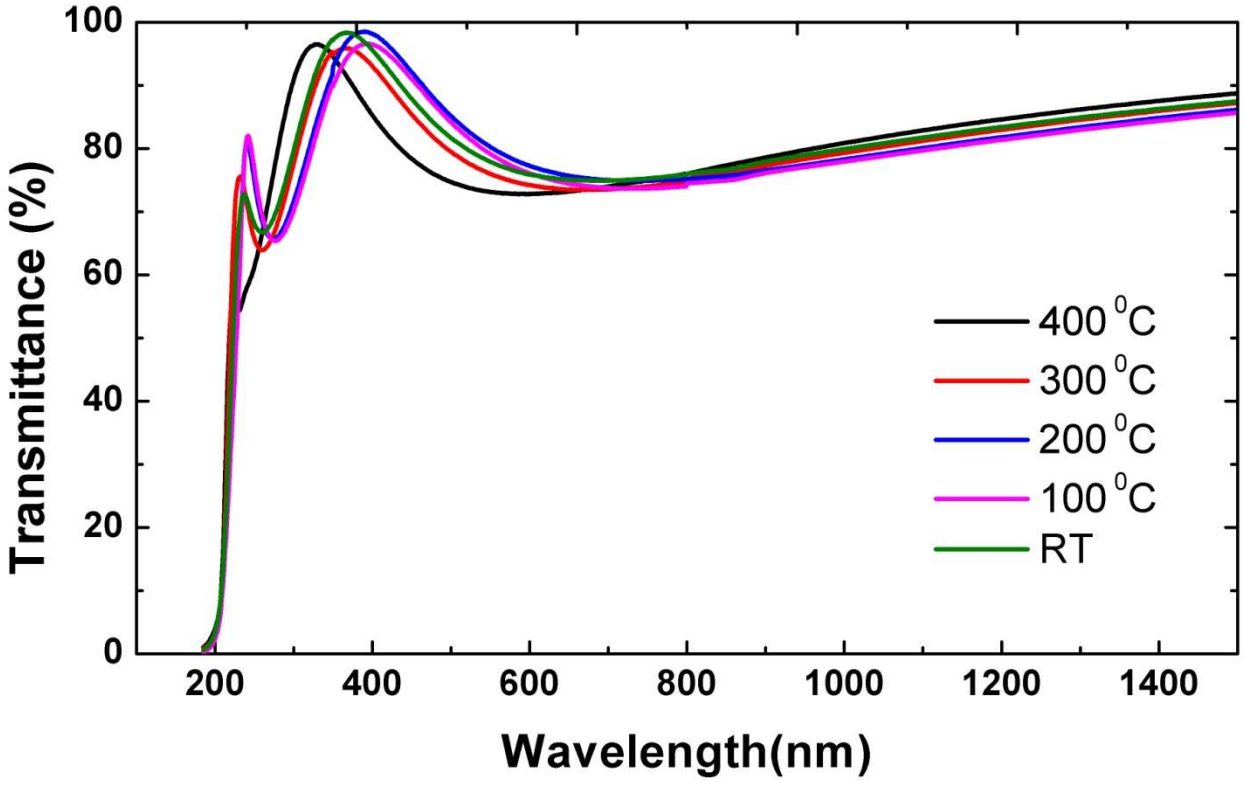

Figure 4.17: Optical transmission spectra of samples of ZrO_2 films (refer Table3.2)

The optical absorption coefficient and, hence, the optical band gap of ZrO_2 thin films can be derived from transmittance measurements using the following relation:

$$\alpha t = -\ln\left(\frac{T}{1-R}\right) - - - - - - (4.1) \quad [31]$$

where, α is the optical absorption coefficient, t is the film thickness, T is the transmittance, and R is the reflectance. As suggested for zirconia electronic structure [32], $(\alpha h\nu)^2$ was calculated and $(\alpha h\nu)^2$ vs. hν was plotted. The intercept of slope of the linear part of the curves (as shown in Figure 4.18) will provide

the band gap energy. The values obtained in the present work vary in the range 5.87 - 6.08 eV for ZrO_2 thin films grown at various temperatures. The electronic structure of zirconia can be roughly described as a valence band formed by the filled O 2p orbital and a conduction band formed by the empty Zr 4d metal levels (Figure 4.19).

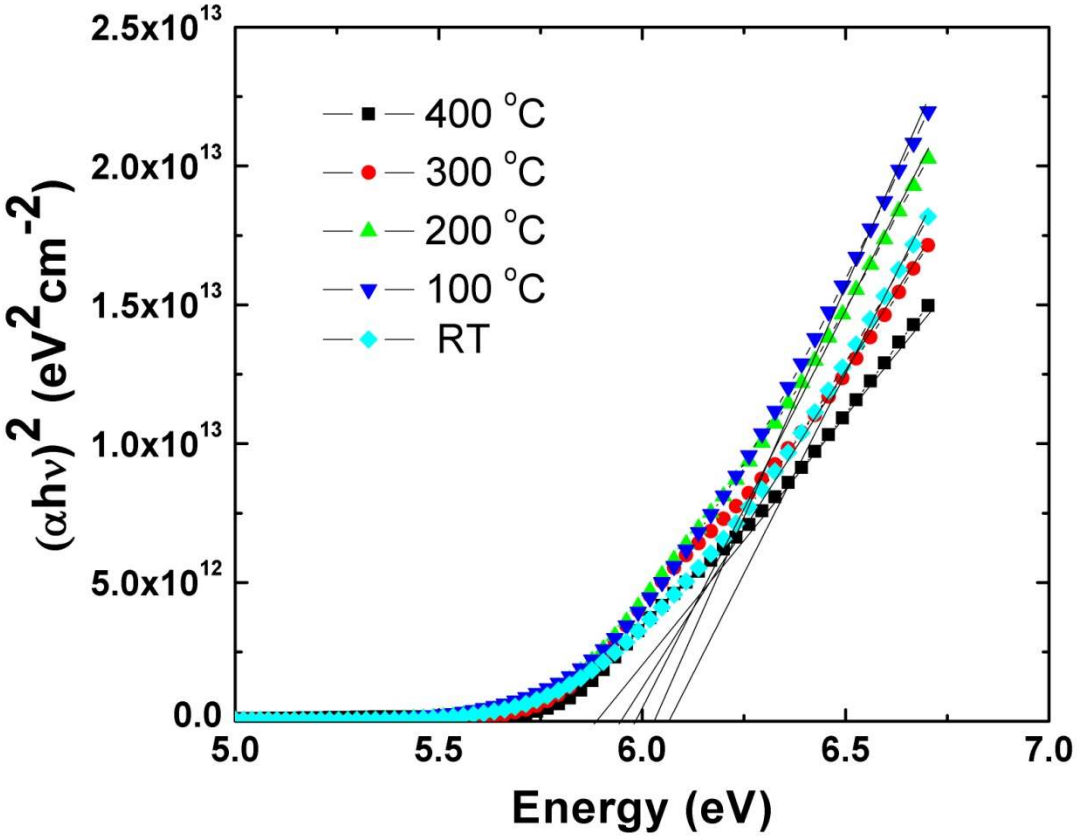

Figure 4.18: $(\alpha h\nu)^2$ vs. hν plot of ZrO_2 samples deposited on quartz substrates

Therefore, the measured band gap in our experiments corresponds to electronic transitions from the top of valence band (band formed by O 2p levels) to the top of the conduction band (formed by Zr 4d levels). It is important to mention that the values obtained in the present work are in close agreement with the reported values in the literature [16-20].

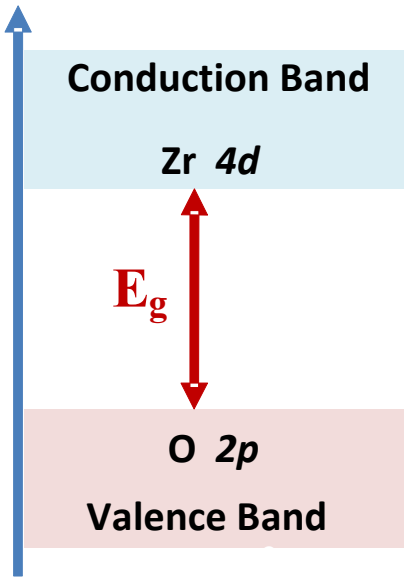

Figure 4.19: Electronic band transitions and band gap of ZrO_2

4.7 The C-V curves

The capacitance density vs. voltage curves of ZrO_2 films (samples ZrOAC1.1 and ZrOAC1.2) are shown in Figs. 20 and 21. The MOS capacitors made out of oxide film grown under same experimental conditions and with a film thickness of 40 nm. The only difference is that one sample is as grown and the other is annealed in a forming gas as described in experimental section. The C-V curves show that the capacitance density is very low for sample without annealing (ZrOAC1.1). It can be noticed that the capacitance is very high (10 times compared that of sample without annealing) for annealed sample (ZrOAC1.2). This indicates that annealing improves the capacitance density. Dielectric constant is calculated using simple capacitor approximation

$$\kappa = \frac{C\, t_{ox}}{\varepsilon_o} = \ 17 \quad ---------(4.2)$$

where C = capacitance density in accumulation region of C-V curve, t_{ox} = thickness of oxide = 42 nm,

The C-V curve of the annealed ZrO_2 film (ZrOAC1.2) indicates a shift to the left by~ 4V. This can be accounted for an increase in interface traps with annealing [33].

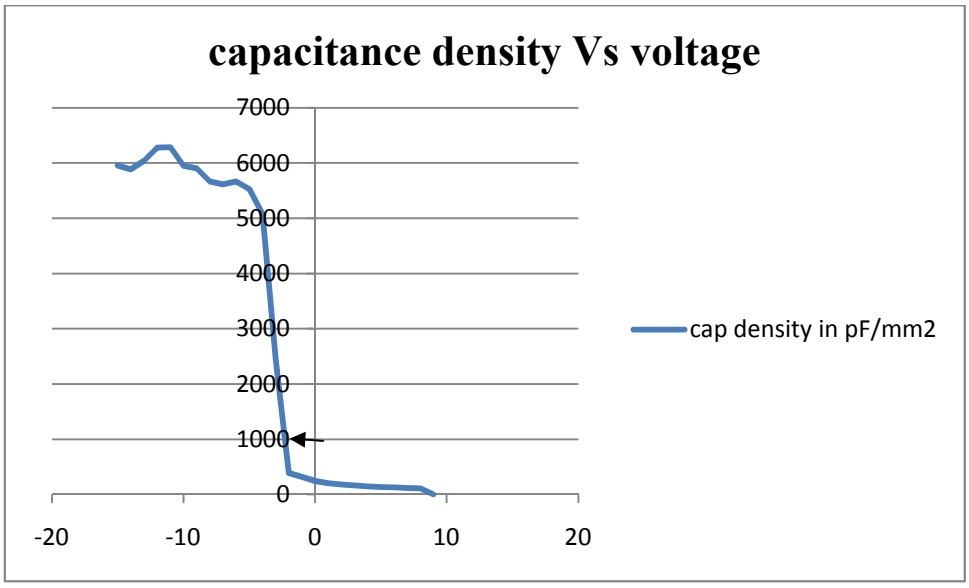

Figure 4.20: Capacitance density of ZrOAC1.2 (annealed sample)

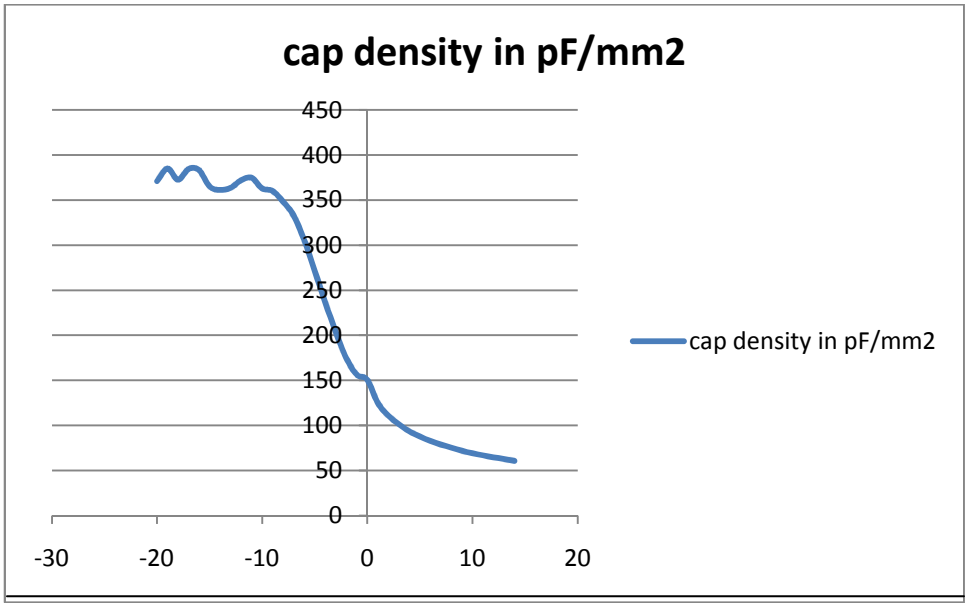

Figure 4.21: Capacitance density of ZrOAC1.1 (not annealed sample)

Chapter 5: Conclusions

ZrO_2 films were grown at various temperatures using magnetron sputtering. The growth behavior, surface structure and morphological features, interface structure, and chemical analysis of surfaces and interfaces have been examined by the high-resolution transmission electron microscopy (HRTEM) and high-resolution scanning electron microscopy (HR-SEM). The crystal structure and interface analysis has been performed using x-ray diffraction (XRD) and x-ray reflectivity (XRR). The optical and electrical properties were evaluated by studying the optical absorption and capacitance-voltage measurements, respectively.

The results indicate that the effect of T_s on the surface structure, interface layers and morphology of ZrO_2 films is significant. ZrO_2 films grown at 30 ^oC are nano-crystalline with a very thin (2.6 nm) interface layer (IL) formation. The grain sizes determined are in the range 5-40 nm, where the temperature-dependence is clear. Films grown at room temperature showed only a 2.6 nm thick IL formation for a film of 145 nm ZrO_2 on Si.

ZrO_2 films grown at $T_s \leq 200$ ^oC are nano-crystalline and exhibit a cubic phase. Stabilization of this cubic phase at lower temperatures is an interesting phenomenon, as the cubic phase of ZrO_2 is a high temperature phase. However, the cause for such phenomenon is yet to be understood. From XRR data it can be concluded that at high temperatures the IL formation is significant. The films grown at high-temperature polymorph (cubic phase), they can be used for high temperature coatings. Computations might provide a much better understanding of the surface energetic, phase stabilization and could be the opportunity for future work. The films are nano-crystalline and dense (non-porous). The optical band gap varies in the range of 5.81-6.02 eV. With the band edge in UV region, these films could be could be useful for application in optoelectronic devices and protective dielectric layer coatings. The most important aspects of this study were summarized below.

- The grain structure and size of the films change depending on deposition substrate temperature. The temperature affects the energetics of interface layer formation, crystal structure and grain formation mechanisms.
- All the films deposited at different substrate temperatures were nano-crystalline and the average grain size varies from 5 to 40 nm.
- From XRR data, it is found that with the increase in substrate temperature, there is an increase in interface layer width. The two-layer concept becomes dominant at $T_s \geq 300\ ^oC$.
- The cross-section TEM and STEM-EDX quantified the interface layer thickness as 2.68 nm for films grown at RT.
- The composition of the interface layer is close to zirconium silicide.
- Optical band gap of ZrO_2 films calculated from spectrophotometry measurements vary from 5.81 eV to 6.02 eV depending on the T_s.
- Interface defect density is increased with the annealing of the films.

References

1. R. R. Schller, "Moore's law, past, present and future", *IEEE spectrum* **34**(1998) 52-59.
2. ITRS 2003 roadmap executive summary , www.itrs.org
3. Sung-Mo Kang, Yusuf Leblebici, CMOS digital integrated circuits, Mc Graw Hill, 2003.
4. George W Hanson, fundamentals of nanoelectronics, Pearson prentice hall, 1st edition, 2008
5. R. Degraeve, G. Grokensen, R. Bellens, M.Depas, H.E. Maes. "A consistent model for thickness dependence of intrinsic breakdown in ultra-thin oxides", *Technical digest of international electron devices meeting* 1995, 863-867.
6. H.J. Hubbard and D.G. Schlom, "Thermodynamic stability of binary oxides in contact with silicon", *Journal of Materials Research* **11** (1996) 2757-2766.
7. Hyoungsub Kim, Ann Marshall, Paul. C. McIntyre, Krishna .C. Saraswat, "Crystallization kinetics and microstructure – dependent leakage current behavior ultrathin HfO_2 dielectrics", *Applied Physics letters* **84** (2004) 2064 - 2068.
8. R.M.C. Almeida, I.J.R. Baumval," Oxygen diffusion: High K gate dielectrics", IOP publishing ltd, 2004.
9. NIST database on ceramics, http://www.ceramics.nist.gov/srd/summary/ftzrtzp.htm.
10. R,S Lima, A Kucuk and C.C. berndt , "Evaluation of micro hardness and elastic modulus of thermally sprayed nano structured zirconia coatings", *Surface coatings and technology* **135** (2001) 166 -172.
11. J. Robertson, Band offsets of wide band gap oxides and implications for future electronic devices, *Journal of Vacuum Science and Technology*. **18** (2000) 1785.
12. G. D. Wilk, R.M. Wallace, J.M Anthony, "High dielectric constant oxides: current status and materials properties considerations", *Journal of Applied Physics*, **89** (2001) 5243 – 5275.

13. J.P.Maria et al, "High temperature stability in lanthanum and zirconia based gate dielectrics", *Journal of Applied Physics* **90 (**2001) 448- 453.
14. Kaupo Kukli, Mikko Ritala, Jaan Aari, Teet Uustare and Markku leskelä, "Influence of growth temperature on properties of zirconium dioxide films grown by atomic layer deposition", *Journal of Applied Physics* **92** (2002) 1833-1840.
15. Michel Cassir, Fabrice Goubin, Cécile Bernay, Philippe Vernoux and Daniel lincot, "Synthesis of ZrO_2 thin films by atomic layer deposition: growth kinetics, structural and electrical properties", *Applied Surface Science* **193** (2002) 120-128.
16. S. Chatterjee, S.K. Samanta, H.D. Banerjee and C.K. Maiti, "Metallo-organic compound-based plasma enhanced CVD of ZrO_2 films for microelectronic applications", *Bulletin of Materials Science*, **24** (2001) 579-582.
17. M. Filipescu, N. Scarisoreanu, V. Craciun, B. Mitu, A. Purice, A. Moldovan, V. Ion, O. Toma and M. Dinescu, "High-κ dielectric oxides obtained by PLD as solution for gates dielectric in MOS devices", *Applied Surface Science* **253** (2007) 8184-8191.
18. Mehmet Alper Sahiner, Joseph C. Woicik, Peng Gao, Patrick McKeown, Mark C. Croft, Michael Gartman and Brendan Bemapfla, "Pulsed laser deposition and characterization of Hf-based high-κ dielectric thin films", *Thin solid films* **515** (2007) 6548-6551.
19. Akira Sawa, Kazuki Nakanishi and Teiichi Hanada, "Preparation and properties of radiofrequency sputtered X-ray amorphous films in the system SiO_2-ZrO_2", *Thin solid films* **516** (2008) 4665-4672.
20. S. Zhao, F. Ma, Z. Song, K. Xu, "Thickness-dependent structural and optical properties of sputter deposited ZrO2 films", *Optical Materials* **30**(2008) 1910 -1915.
21. H.S. Choi, K.S. Seol, D.Y. Kim, J.S. Kwak, C.S. Son, I.H. Choi, "Thermal treatment effects on interfacial layer formation between ZrO_2 thin films and Si substrates", *Vacuum* **80** (2005) 310-316.

22. Li min chen, Yi Sheng Lai and J.S. chen, "Influence of pre deposition treatments on interfacial and electrical characteristics of ZrO_2 gate dielectrics", *Thin Solid Films* **515** (2007) 3724 – 3729.
23. Crystallography open database, www.crystallography.net.
24. Wyckoff R W G, "Fluorite structure: Crystal Structures", Second edition, Inter science Publishers, New York, 1963.
25. K.Y Takeda and H. Arashi, "In situ determination of crystal structure for high pressure phase of ZrO_2 using a diamond anvil and single crystal X-ray diffraction method Sample: P = 15 kbar", *Physics and Chemistry of Minerals* **13** (1986) 233 – 237.
26. M. Yoshimura, "Phase Stability of Zirconia", *American Ceramic Society Bulletin* **67**(1988) 1950-1955.
27. Aldebert, J.P. Traverse, "Structure and Ionic Mobility of Zirconia at High Temperature", *Journal of American Ceramic Society* **68** (1985) 34-37.
28. R.N. Patil, E.C. Subbarao, "Axial thermal expansion of zro2 and hfo2 in the range room temperature to 1400°C", *Journal Applied Crystallography* **2** (1969) 281-286.
29. E.C. Subbarao, H.S. Maiti, K.K. Srivastava, "Martenstic transformation in zirconia", *Physica Status Solidi A* **21**(1974) 9-13.
30. R.C. Garvie, R.H.J. Hannink, R.T. Pascoe, "Ceramics Steel", *Nature* **258** (1975) 703-708.
31. V. Srikant, D. R. Clarke, "On the optical band gap of zinc oxide", *Journal of applied physics* **83** (1998) 5447-5451.
32. A.S. Foster, V.B. Sulimov, F. Lopez Gejo, A.L. Schluger, R.M. Nieminen, "Modeling of point defects in monoclinic zirconia", *Physical Review B* **64** (2001) 224108.
33. S. M. Sze, "Semiconductor devices: physics and technology", first edition, John Wiley & Sons, 1985.

Vita

First Son of Sri Rama Murthy Vemuri and Naga Rajeswari, Venkata Rama Sesha Ravi Kumar Vemuri was born in Eluru, West Godawari, India, on 26th of February, 1982. He has one brother and three sisters. He Graduated from J N T University with a Bachelor of Technology in Electrical Engineering in first division and traveled to The University of Texas at El Paso to pursue a Master of Science Electrical Engineering. While working towards Masters Degree, he worked as teaching assistant in electrical and computer engineering department and graduate research assistant at NanoMIL. Now, he is a member of Energy Systems Laboratory at UTEP. During summer2007 he worked as an intern at International SEMATECH as defect metrology engineering intern. In fall 2009, he graduated from Master of Science in electrical engineering and proceeded further to pursue interdisciplinary ESE PhD program at UTEP.

Permanent address: D. No 34 – 11- 4

Vankavari veedhi

Tanuku, 534211, India

This Thesis was typed by Venkata Rama Sesha Ravi Kumar Vemuri